Uptake of Cefazolin and Phenolsulfonphthalein by HEK293 Cells Transfected with hOAT1 or hOAT3 cDNA

For the uptake study of cefazolin and phenolsulfonphthalein, HEK293 cells were seeded on 6-cm poly-D-lysine-coated dish at a density of 2×10^6 cells/dish and then transfected with 8 μg hOAT1 or hOAT3 cDNA per dish at 24 h after seeding. At 48 h after transfection, the uptake studies of cefazolin and phenolsulfonphthalein were performed. The cells were preincubated with 2 ml of incubation medium for 10 min. After the preincubation, the medium was replaced with 2 ml of the incubation medium containing 200 μM cefazolin or 500 μM phenolsulfonphthalein. At the end of the 1-h incubation period, the medium was aspirated, and cells were washed once with 5 ml of ice-cold incubation medium containing 2% bovine serum albumin, and then four times with bovine serum albumin free ice-cold incubation medium. For measurement of the cefazolin accumulation, the cells were scraped and homogenized with 1 ml water. With 5 μl of the homogenate, protein contents were determined. To 0.98 ml of the homogenate, 20 μl of phosphoric acid was added and mixed for 30 s, then the samples were loaded onto an Oasis HLB cartridge (Waters Corporation, Milford, MA, USA) preconditioned with 1 ml each of methanol and water. The column was then washed with 1 ml of 5% methanol and then cefazolin was eluted from the column by 1 ml of methanol. The eluate was evaporated to bare dryness at 45–50°C and resuspended in 200 μl of mobile phase buffer, and the solution was filtered through a 0.45-μm polyvinylidene fluoride filter. The concentration of cefazolin was measured with HPLC under the following conditions: mobile phase, 30 mM phosphate buffer (pH 5.2):methanol = 88:12; flow rate, 1.0 ml/min; wavelength, 272 nm; temperature, 40°C. For measurement of the phenolsulfonphthalein accumulation, the cells were scraped with 1.5 ml of 75% ethanol, incubated for 1 h at room temperature, and centrifuged at 3000g for 10 min. After centrifugation, 1 ml of the supernatant was alkalized with 100 μl of 1 N NaOH and the concentration of phenolsulfonphthalein was determined spectrophotometrically at 546 nm. The pellet was solubilized with 1 ml of 1 N NaOH and protein contents were determined.

Statistical Analysis

Data were analyzed statistically using nonpaired *t* test or the one-way analysis of variance followed by Scheffe's test.

Materials

p-[Glycyl-^{14}C]aminohippurate (1.9 GBq/mmol) was purchased from Du Pont-New England Nuclear Research Product (Boston, MA, USA). [6,7-^{3}H(N)]Estrone sulfate ammonium salt (1.9 TBq/mmol) was obtained from Perkin Elmer Life Sciences (Boston, MA, USA). Cefazolin (Fujisawa Pharmaceutical Co., Osaka, Japan) was from the source. All other chemicals used were of the highest purity available.

RESULTS

Quantification of hOAT1, hOAT2, hOAT3, and hOAT4 mRNA Levels in the Normal Human Kidney Cortex and Renal Biopsy Samples

To investigate the expression levels of renal organic anion transporters, we performed quantitative real-time PCR. Fig. 1 shows the mRNA levels of organic anion transporters in normal parts of the renal cortex or the renal biopsy specimens from patients with kidney diseases. Only the level of hOAT1 mRNA in the renal biopsy specimens was significantly lower than that in the normal control ($p < 0.05$). The level of hOAT3 mRNA was slightly decreased, although the levels of hOAT2 and hOAT4 mRNA were increased in biopsy sections compared with each mRNA level in the normal kidney (differences not significant).

Correlation Between the Elimination Rate of Cefazolin and PSP15′, PSP120′, CL_{cr}, or Expression Levels of Organic Anion Transporters

Fig. 2 shows the linear regression of Ke_{cez} against PSP15′ (A), PSP120′ (B), or CL_{cr} (C) and the relation between CL_{cr} and PSP15′ (D) or PSP120′ (E). Although we detected a poor correlation between Ke_{cez} and CL_{cr} ($r = 0.40$, $p < 0.05$), there was a good linear correlation between Ke_{cez} and PSP15′ ($r = 0.75$, $p < 0.01$) or PSP120′ ($r = 0.67$, $p < 0.01$). However, there was a poor correlation between CL_{cr} and PSP15′ ($r = 0.48$, $p < 0.05$) or PSP120′ ($r = 0.56$, $p < 0.01$).

Fig. 3 shows the correlation between the Ke_{cez} and mRNA levels of organic anion transporters. The levels of hOAT3 mRNA was significantly correlated with the Ke_{cez} ($r = 0.44$, $p < 0.05$), although there was no correlation between hOAT1, hOAT2, or hOAT4 mRNA levels and Ke_{cez}.

Characterization of Organic Anion Uptake in HEK293 Cells Transfected with hOAT1 or hOAT3 cDNA

Good linear correlation between Ke_{cez} and PSP15′ or PSP120′ suggested that both cefazolin and phenolsulfonphthalein were excreted via the same organic anion transporters in the renal tubules. Therefore, we investigated the effects of cefazolin or phenolsulfonphthalein on the hOAT1 and hOAT3 transport activities. The transport function of hOAT1 and hOAT3 was assessed by the uptake of *p*-[^{14}C]aminohippurate and [^{3}H]estrone sulfate in HEK293 cells, respectively. Fig. 4 shows the time course of *p*-aminohippurate or estrone sulfate uptake by hOAT1- or hOAT3-expressing HEK293 cells. The accumulations of *p*-aminohippurate and estrone

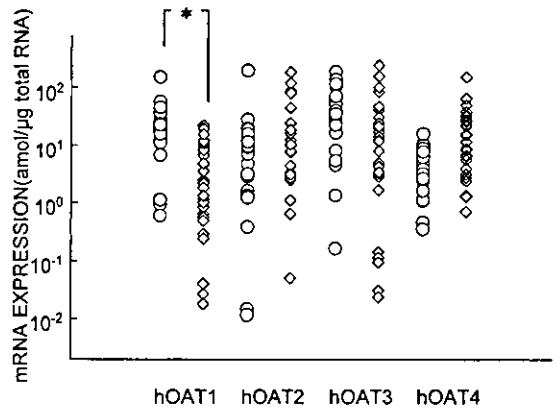

Fig. 1. Expression levels of hOAT1, hOAT2, hOAT3, and hOAT4 mRNA in the human kidney. Total cellular RNA was extracted from normal human kidney cortex (○) and renal biopsy specimens of patients with renal diseases (◇). The mRNA levels of these transporters were determined by real-time PCR. *$p < 0.05$, significant difference.

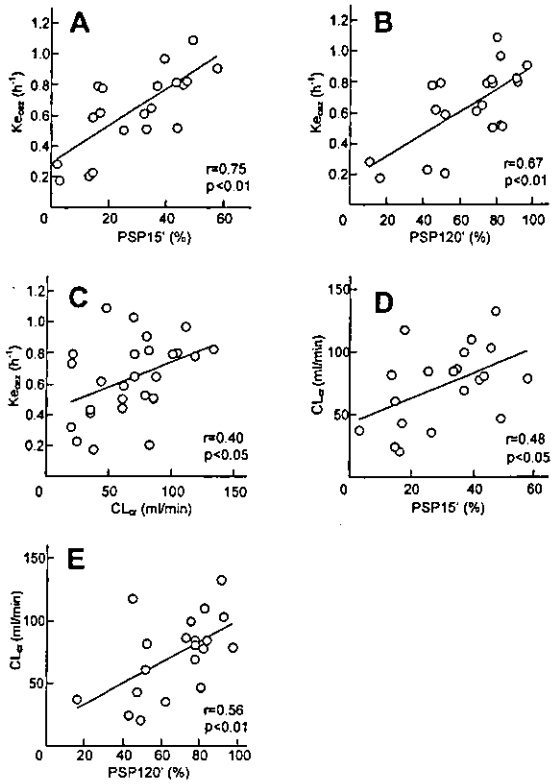

Fig. 2. The linear regression of the elimination constant of cefazolin against the 15- (A) or 120-min (B) values of the phenolsulfonphthalein test or creatinine clearance (C), and the relationship between creatinine clearance and 15- (D) or 120-min (E) values of the phenolsulfonphthalein test. The plasma concentration of cefazolin was measured by HPLC, and elimination constant of cefazolin (Ke_{cez}) was calculated.

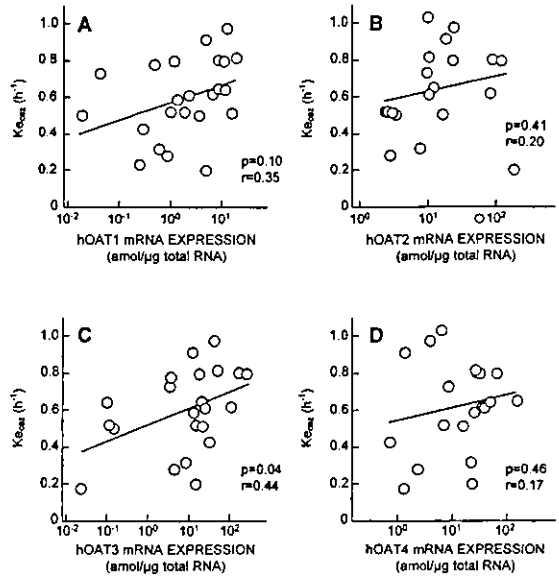

Fig. 3. The linear regression of Ke_{cez} against hOAT1 (A), hOAT2 (B), hOAT3 (C), and hOAT4 (D) mRNA levels. The plasma concentration of cefazolin was measured by HPLC, and Ke_{cez} was calculated. Total cellular RNA was extracted from the kidney biopsy specimens. The mRNA levels of hOAT1, hOAT2, hOAT3, and hOAT4 were quantified by real-time PCR.

sulfate were increased in a time-dependent manner, although the accumulations of these substrates in HEK293 cells, transfected with the blank vector alone, exhibited a negligible increase.

As shown in Fig. 5, a concentration-dependence of *p*-[^{14}C]aminohippurate and [^{3}H]estrone sulfate uptake was observed in hOAT1- and hOAT3-transfected cells. Using a nonlinear least squares regression analysis, kinetic parameters were calculated according to the Michaelis-Menten equation from three separate experiments. Apparent Michaelis-Menten constants (K_m) for *p*-[^{14}C]aminohippurate transport via hOAT1 and for [^{3}H]estrone sulfate transport via hOAT3 were 47.8 ± 19.5 and 6.6 ± 3.0 μM (mean ± SE), respectively, which were consistent with previous report (17). Maximal uptake rate (V_{max}) values for hOAT1 and hOAT3 were 305.7 ± 95.4 and 44.2 ± 8.1 pmol/mg protein/min (mean ± SE), respectively.

Fig. 6 shows that the effects of cefazolin or phenolsulfonphthalein on the hOAT1 or hOAT3 transport activity. Both cefazolin and phenolsulfonphthalein inhibited the organic anion uptake by hOAT1- and hOAT3-transfected cells, respectively, in a dose-dependent manner. The IC_{50} values were estimated by nonlinear regression analysis of the competition curves with one compartment model with the following equation: $V = 100 \times IC_{50} / (IC_{50} + [I]) + A$, where V is the uptake amount (% of control), $[I]$ is the concentration of cefazolin or phenolsulfonphthalein, and A is the nonspecific organic anion uptake (% of control). The IC_{50} values for cefazolin and phenolsulfonphthalein on hOAT1-mediated *p*-aminohippurate uptake were 100.6 ± 25.3 μM and 8.1 ± 1.3 μM, respectively, and the IC_{50} values for cefazolin and phenolsulfonphthalein on hOAT3-mediated estrone sulfate uptake were 116.6 ± 13.0 μM and 66.0 ± 16.5 μM, respectively.

Uptake of Cefazolin and Phenolsulfonphthalein by hOAT1- and hOAT3-Expressing HEK293 Cells

To investigate whether cefazolin and phenolsulfonphthalein are the substrates for hOAT1 and hOAT3, we measured the accumulation of cefazolin and phenolsulfonphthalein in hOAT1- and hOAT3-expressing HEK293 cells. The cefazolin accumulation in hOAT3-expressing HEK293 cells was significantly higher than that in control cells and the uptake of

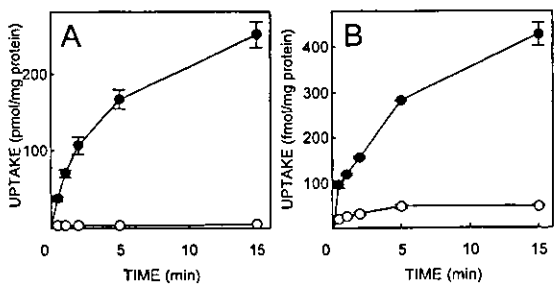

Fig. 4. Time course of *p*-[^{14}C]aminohippurate and [^{3}H]estrone sulfate accumulation in HEK293 cells. (A) *p*-[^{14}C]aminohippurate accumulation in HEK293 cells transfected with pBK-CMV vector (○) or hOAT1 (●) cDNA. The cells were incubated with 5 μM *p*-[^{14}C] aminohippurate at 37°C for specified periods. (B) [^{3}H] estrone sulfate accumulation in HEK293 cells transfected with pBK-CMV vector (○) or hOAT3 (●) cDNA. The cells were incubated with 18.8 nM [^{3}H]estrone sulfate at 37°C for specified periods. Each point represents the mean ± SE of three monolayers

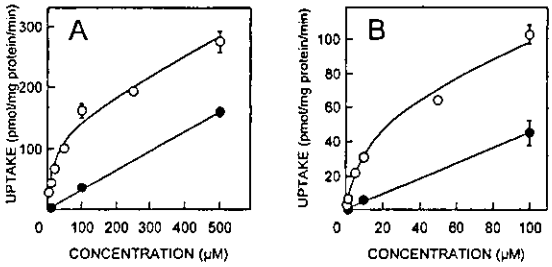

Fig. 5. Concentration dependence of *p*-[^{14}C]aminohippurate (A) and [^{3}H]estrone sulfate (B) accumulation in HEK293 cells transfected with hOAT1 or hOAT3 cDNA, respectively. The cells transfected with hOAT1 or hOAT3 cDNA were incubated with various concentrations of *p*-[^{14}C]aminohippurate (A) or [^{3}H]estrone sulfate (B) in the absence (○) or presence (●) of unlabeled 5 mM *p*-aminohippurate (A) or 1 mM estrone sulfate (B) at 37°C for 1 min. After incubation, radioactivity of solubilized cells was measured. Each point represents the mean ± SE of nine monolayers from three separate experiments.

cefazolin by hOAT3 was inhibited by phenolsulfonphthalein similar to the level of controls (Fig. 7A). In contrast, hOAT1-mediated cefazolin transport was not detected. We confirmed hOAT1-mediated *p*-aminohippurate uptake and hOAT3-mediated estrone sulfate uptake in the same transfected cells (Figs. 7B and C). As shown in Fig. 8, furthermore, the phenolsulfonphthalein accumulations in both hOAT1- and hOAT3-expressing HEK293 cells were significantly higher than those in control cells, and cefazolin inhibited the phenolsulfonphthalein uptake by both cells to the control level.

DISCUSSION

Renal secretion of various drugs is mediated by the drug transporters expressed in the tubular epithelial cells, and the alteration of these transporter levels may affect the drug elimination by the kidney. In the present study, the expression levels of organic anion transporters in kidney diseases were quantified to compare with those in normal controls, and then correlations between the mRNA levels of these transporters and anionic drug excretion were analyzed.

The mRNA level of hOAT1 in biopsy samples of patients with renal diseases was lower than that in the normal kidney cortex (Fig. 1). Although the level of hOAT3 mRNA also tended to decrease, the levels of hOAT2 and hOAT4 mRNA were apt to increase. Recently, we reported the alteration of the renal transporter expression in 5/6 nephrectomized rats, which have been widely used to study the progression of renal damage resulting from reduction of nephron mass (18–20). Rat organic cation transporter OCT2 protein was markedly decreased and H^+/peptide cotransporter PEPT2 protein was significantly increased in the kidney of these rats. Moreover, other transporters were not changed

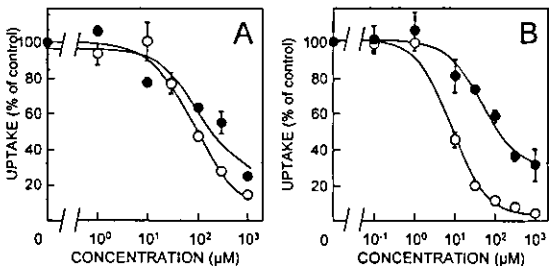

Fig. 6. Effects of cefazolin (A) or phenolsulfonphthalein (B) on *p*-[^{14}C]aminohippurate and [^{3}H]estrone sulfate accumulation in HEK293 cells transfected with hOAT1 or hOAT3 cDNA, respectively. Monolayers of hOAT1 (○)- or hOAT3 (●)-expressing HEK293 cells were incubated for 1 min at 37°C with 5 μM *p*-[^{14}C]aminohippurate (○) or 18.8 nM [^{3}H]estrone sulfate (●) in the presence of various concentrations of cefazolin or phenolsulfonphthalein. After incubation, the radioactivity of solubilized cells was measured. Each point represents the mean ± SE of nine monolayers from three separate experiments.

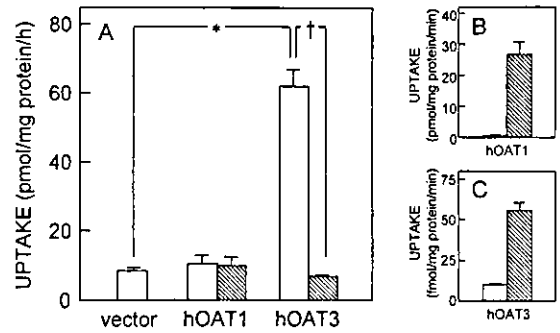

Fig. 7. Uptake of cefazolin in hOAT1 or hOAT3 transfected HEK293 cells. (A) Monolayers of hOAT1- or hOAT3-expressing HEK293 cells were incubated for 1 h at 37°C with 200 μM cefazolin in the absence (open columns) or presence (hatched columns) of 3 mM phenolsulfonphthalein. After incubation, the accumulation of cefazolin in the cells was measured by HPLC. (B) *p*-[^{14}C]aminohippurate accumulation in HEK293 cells transfected with pBK-CMV vector (open column) or hOAT1 (hatched column) cDNA. (C) [^{3}H]estrone sulfate accumulation in HEK293 cells transfected with pBK-CMV vector (open column) or hOAT3 (hatched column) cDNA. The cells were incubated with 5 μM *p*-[^{14}C]aminohippurate or 18.8 nM [^{3}H]estrone sulfate at 37°C for 1 min. Each column represents the mean ± SE of three monolayers. *p < 0.01, †p < 0.01, significant differences.

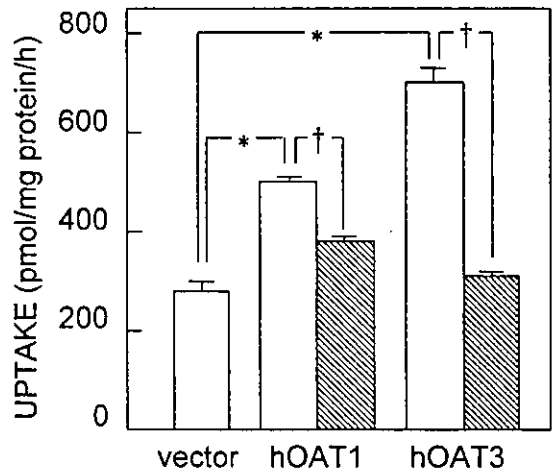

Fig. 8. Uptake of phenolsulfonphthalein in hOAT1 or hOAT3 transfected HEK293 cells. Monolayers of hOAT1- or hOAT3-expressing HEK293 cells were incubated for 1 h at 37°C with 500 μM phenolsulfonphthalein in the absence (open columns) or presence (hatched columns) of 10 mM cefazolin. After incubation, the accumulation of phenolsulfonphthalein in the cells was measured spectrophotometrically. Each column represents the mean ± SE of three monolayers. *p < 0.01, †p < 0.01, significant differences.

significantly. It was suggested that each transporter underwent a different effect in the impaired kidney.

In our previous study, we demonstrated that hOAT1 and hOAT3 could be major transporters in the human kidney cortex and localized at the basolateral membrane of the proximal tubular cells (10). Because hOAT1 and hOAT3 may play important roles in renal anion secretion, it was assumed that the changes in these expression levels affected renal drug secretion. In this study, cefazolin was selected to evaluate renal drug secretion, because it was reported that tubular secretion amounted to 50-80% of total excreted cefazolin in the patients with a glomerular filtration rate above 25 ml/min (21). In addition, the cefazolin elimination rate was significantly decreased by co-administration of probenecid to about 60% (22), suggesting that cefazolin was secreted by anion transport systems. Indeed, the Ke_{cez} varied among the patients. While no correlation could be found between the elimination rate of cefazolin (Ke_{cez}) and hOAT1, hOAT2 or hOAT4 expression levels, there is a significant correlation between Ke_{cez} and hOAT3 mRNA levels (Fig. 3). Although renal drug excretion is affected by many factors, such as glomerular filtration rate, renal blood flow rate, protein binding and transport abilities of tubular epithelial cells, the expression levels of transporters may be concerned mainly with transport capacities of epithelial cells. In addition, the patients in this study had various renal diseases and stages. Further investigation is needed to clarify more precise correlation between expression levels of transporters and renal drug secretion. So far, present results suggested that the renal excretion of the cefazolin was partly affected by hOAT3 expression levels.

The elimination rate of cefazolin was correlated with the urinary excretion of phenolsulfonphthalein (Fig. 2), suggesting that these compounds were excreted through common transporters. However, it was not certain which transporter mediated the secretion of these drugs in the human kidney. Phenolsulfonphthalein is mainly secreted from the kidney, and is often used for the diagnosis of renal function. It was reported that the accumulation of phenolsulfonphthalein into the renal tubules was inhibited by anionic compounds such as probenecid or 2,4-dinitrophenol (23). Therefore, tubular secretion of phenolsulfonphthalein should be mediated by the anion transport system (4). Hosoyamada *et al.* reported that phenolsulfonphthalein inhibited p-aminohippurate transport by hOAT1 (8). In this study, we confirmed that phenolsulfonphthalein inhibits the hOAT1-mediated *p*-aminohippurate transport in a dose-dependent manner. Moreover, it was shown that the phenolsulfonphthalein was transported by hOAT1 and hOAT3 (Fig. 8). Therefore, it is suggested that renal secretion of phenolsulfonphthalein is mediated by these transporters in the normal kidney.

It was reported that cefazolin inhibited the hOAT1- and hOAT3-mediated transport (24–26), and was transported by rOAT1 (27). In the present study, cefazolin inhibited the hOAT1- and hOAT3-mediated uptake, supporting previous finding. However, only hOAT3-mediated cefazolin transport could be detected in the present study (Fig. 7). Since this experiment was performed with higher concentration of cefazolin than IC_{50} value for cefazolin on hOAT1-mediated p-aminohippurate uptake, it could not be denied that cefazolin transport by hOAT1 should be detected at lower concentration. However, it is suggested that cefazolin is more effectively transported by hOAT3 than by hOAT1 and that hOAT3, rather than hOAT1, is the common transport pathway of tubular secretion of phenolsulfonphthalein and cefazolin.

The serum concentration of cefazolin at immediately after the infusion was 101.5 to 431.0 μM (data not shown). Because about 80% of cefazolin bound to the protein (21), the concentration of free serum cefazolin is comparable to IC_{50} value for cefazolin on hOAT3 transport. It is possible that cefazolin is efficiently transported by hOAT3 from blood circulation to tubular epithelial cells.

Patients with chronic renal insufficiency or nephritic syndrome frequently manifest diuretic resistance. It was suggested that the carrier-mediated tubular secretion of diuretics is important for its efficacy (28,29). In a previous study, we suggested that rOAT1 contributes, at least in part, to renal tubular secretion of acetazolamide, thiazides, and loop diuretics (30). In the present study, the hOAT1 mRNA level in the renal diseases was lower than that of normal parts of the kidney. It is possible that diuretic resistance may be partly due to the reduction of tubular secretion by the decreased hOAT1 expression.

This is the first report showing the expression profile of renal drug transporters in patients with kidney diseases and provided novel information as follows. Firstly, the hOAT1 mRNA levels in the kidney of patients with renal diseases were lower than in the normal kidney cortex. Secondly, renal excretion of the anionic drug cefazolin was significantly correlated with hOAT3 mRNA levels in patients with renal diseases. Thirdly, both phenolsulfonphthalein and cefazolin were transported by hOAT3. These results suggested that hOAT3 should play an important role on the secretion of these anionic drugs in patients with renal diseases. Although further investigation is needed to apply the expression levels of drug transporters to dosage adjustment, it is possible that the expression profiles of drug transporters may be useful information for understanding the alteration of renal drug secretion.

ACKNOWLEDGMENTS

This work was supported by a grant-in-aid for Research on Human Genome, Tissue Engineering and Food Biotechnology from the Ministry of Health, Labor and Welfare of Japan (H12-Genome-019) and a grant-in-aid for Scientific Research from the Ministry of Education, Culture, Sports, Science and Technology of Japan.

REFERENCES

1. L. Dettli. Drug dosage in renal disease. *Clin. Pharmacokinet.* **1**:126–134 (1976).
2. R. Hori, K. Okumura, A. Kamiya, H. Nihira, and H. Nakano. Ampicillin and cephalexin in renal insufficiency. *Clin. Pharmacol. Ther.* **34**:792–798 (1983).
3. R. Hori, K. Okumura, H. Nihira, H. Nakano, K. Akagi, and A. Kamiya. A new dosing regimen in renal insufficiency: application to cephalexin. *Clin. Pharmacol. Ther.* **38**:290–295 (1985).
4. J. V. Moller and M. I. Sheikh. Renal organic anion transport system: pharmacological, physiological, and biochemical aspects. *Pharmacol. Rev.* **34**:315–358 (1982).
5. G. Burckhardt and N. A. Wolff. Structure of renal organic anion and cation transporters. *Am. J. Physiol. Renal Physiol.* **278**:F853–F866 (2000).

6. K. Inui, S. Masuda, and H. Saito. Cellular and molecular aspects of drug transport in the kidney. *Kidney Int.* **58**:944–958 (2000).
7. T. Sekine, S. H. Cha, and H. Endou. The multispecific organic anion transporter (OAT) family. *Pflugers Arch.* **440**:337–350 (2000).
8. M. Hosoyamada, T. Sekine, Y. Kanai, and H. Endou. Molecular cloning and functional expression of a multispecific organic anion transporter from human kidney. *Am. J. Physiol.* **276**:F122–F128 (1999).
9. R. Lu, B. S. Chan, and V. L. Schuster. Cloning of the human kidney PAH transporter: narrow substrate specificity and regulation by protein kinase C. *Am. J. Physiol.* **276**:F295–F303 (1999).
10. H. Motohashi, Y. Sakurai, H. Saito, S. Masuda, Y. Urakami, M. Goto, A. Fukatsu, O. Ogawa, and K. Inui. Gene expression levels and immunolocalization of organic ion transporters in the human kidney. *J. Am. Soc. Nephrol.* **13**:866–874 (2002).
11. A. Enomoto, M. Takeda, M. Shimoda, S. Narikawa, Y. Kobayashi, T. Yamamoto, T. Sekine, S. H. Cha, T. Niwa, and H. Endou. Interaction of human organic anion transporters 2 and 4 with organic anion transport inhibitors. *J. Pharmacol. Exp. Ther.* **301**: 797–802 (2002).
12. S. H. Cha, T. Sekine, J. Fukushima, Y. Kanai, Y. Kobayashi, T. Goya, and H. Endou. Identification and characterization of human organic anion transporter 3 expressing predominantly in the kidney. *Mol. Pharmacol.* **59**:1277–1286 (2001).
13. D. H. Sweet, D. S. Miller, J. B. Pritchard, Y. Fujiwara, D. R. Beier, and S. K. Nigam. Impaired organic anion transport in kidney and choroid plexus of organic anion transporter 3 (Oat3 (Slc22a8)) knockout mice. *J. Biol. Chem.* **277**:26934–26943 (2002).
14. E. Babu, M. Takeda, S. Narikawa, Y. Kobayashi, A. Enomoto, A. Tojo, S. H. Cha, T. Sekine, D. Sakthisekaran, and H. Endou. Role of human organic anion transporter 4 in the transport of ochratoxin A. *Biochim. Biophys. Acta* **1590**:64–75 (2002).
15. Y. Urakami, M. Akazawa, H. Saito, M. Okuda, and K. Inui. cDNA cloning, functional characterization, and tissue distribution of an alternatively spliced variant of organic cation transporter hOCT2 predominantly expressed in the human kidney. *J. Am. Soc. Nephrol.* **13**:1703–1710 (2002).
16. M. M. Bradford. A rapid and sensitive method for the quantitation of microgram quantities of protein utilizing the principle of protein-dye binding. *Anal. Biochem.* **72**:248–254 (1976).
17. M. Takeda, S. Narikawa, M. Hosoyamada, S. H. Cha, T. Sekine, and H. Endou. Characterization of organic anion transport inhibitors using cells stably expressing human organic anion transporters. *Eur. J. Pharmacol.* **419**:113–120 (2001).
18. K. Takahashi, S. Masuda, N. Nakamura, H. Saito, T. Futami, T. Doi, and K. Inui. Upregulation of H^+-peptide cotransporter PEPT2 in rat remnant kidney. *Am. J. Physiol. Renal Physiol.* **281**:F1109–F1116 (2001).
19. A. Takeuchi, S. Masuda, H. Saito, T. Doi, and K. Inui. Role of kidney-specific organic anion transporters in the urinary excretion of methotrexate. *Kidney Int.* **60**:1058–1068 (2001).
20. L. Ji, S. Masuda, H. Saito, and K. Inui. Down-regulation of rat organic cation transporter rOCT2 by 5/6 nephrectomy. *Kidney Int.* **62**:514–524 (2002).
21. E. K. Brodwall, T. Bergan, and O. Ørjavik. Kidney transport of cefazolin in normal and impaired renal function. *J. Antimicrob. Chemother.* **3**:585–592 (1977).
22. G. R. Brown. Cephalosporin-probenecid drug interactions. *Clin. Pharmacokinet.* **24**:289–300 (1993).
23. M. I. Sheikh. Renal handling of phenol red. I. A comparative study on the accumulation of phenol red and p-aminohippurate in rabbit kidney tubules in vitro. *J. Physiol.* **227**:565–590 (1972).
24. S. Jariyawat, T. Sekine, M. Takeda, N. Apiwattanakul, Y. Kanai, S. Sophasan, and H. Endou. The interaction and transport of β-lactam antibiotics with the cloned rat renal organic anion transporter 1. *J. Pharmacol. Exp. Ther.* **290**:672–677 (1999).
25. K. Y. Jung, M. Takeda, M. Shimoda, S. Narikawa, A. Tojo, K. Kim do, A. Chairoungdua, B. K. Choi, H. Kusuhara, Y. Sugiyama, T. Sekine, and H. Endou. Involvement of rat organic anion transporter 3 (rOAT3) in cephaloridine-induced nephrotoxicity: in comparison with rOAT1. *Life Sci.* **70**:1861–1874 (2002).
26. M. Takeda, E. Babu, S. Narikawa, and H. Endou. Interaction of human organic anion transporters with various cephalosporin antibiotics. *Eur. J. Pharmacol.* **438**:137–142 (2002).
27. Y. Uwai, H. Saito, and K. Inui. Rat renal organic anion transporter rOAT1 mediates transport of urinary-extreted cephalosporins, but not of biliary-extracted cefoperazon. *Drug. Metabol. Pharmacokin.* **17**:125–129 (2002).
28. M. Burg, L. Stoner, J. Cardinal, and N. Green. Furosemide effect on isolated perfused tubules. *Am. J. Physiol.* **225**:119–124 (1973).
29. J. F. Seely and J. H. Dirks. Site of action of diuretic drugs. *Kidney Int.* **11**:1–8 (1977).
30. Y. Uwai, H. Saito, Y. Hashimoto, and K. Inui. Interaction and transport of thiazide diuretics, loop diuretics, and acetazolamide via rat renal organic anion transporter rOAT1. *J. Pharmacol. Exp. Ther.* **295**:261–265 (2000).

Available online at www.sciencedirect.com
SCIENCE DIRECT®
Biochemical and Biophysical Research Communications 316 (2004) 416–420
BBRC
www.elsevier.com/locate/ybbrc

Genetic variant Arg57His in human H^+/peptide cotransporter 2 causes a complete loss of transport function

Tomohiro Terada, Megumi Irie, Masahiro Okuda, and Ken-ichi Inui*

Department of Pharmacy, Kyoto University Hospital, Sakyo-ku, Kyoto 606-8507, Japan

Received 11 February 2004

Abstract

We evaluated the functional consequences of genetic variations in human H^+/peptide cotransporter 2 (hPEPT2, *SLC15A2*) resulting in the amino acid changes Arg57His (R57H) and Pro409Ser (P409S). The transport activity of variant R57H was completely abolished, whereas that of variant P409S was comparable with that of wild-type hPEPT2 at pH 5.0–8.0. R57H variant protein was detected in the crude membranes of transiently expressed HEK293 cells by Western blot analysis. The expression of the R57H variant at the plasma membrane was confirmed by indirect immunofluorescence in *Xenopus* oocytes, suggesting that the loss of transport function of hPEPT2 R57H was not due to a change in membrane protein expression. This is the first demonstration of a functional impairment of the SLC15A family induced by a single nucleotide polymorphism.
© 2004 Elsevier Inc. All rights reserved.

Keywords: Peptide transporter; PEPT2; Single nucleotide polymorphism; HEK293; *Xenopus* oocytes

Drug transporters as well as drug-metabolizing enzymes play pivotal roles in determining the pharmacokinetic profiles of drugs and also their pharmacological effects. Recent technological advances such as massive molecular sequencing have allowed the identification of single nucleotide polymorphisms (SNPs) of drug transporters. Evans et al. [1,2] suggested that SNPs of drug transporter genes are responsible for the variation in drug responses among individuals. SNPs in coding regions (cSNPs) of drug transporters are of particular interest, because cSNPs induce amino acid mutations that may alter the function or membrane expression of drug transporters. The functional characterization of drug transporter cSNPs has been reported for human organic cation transporter 1 (hOCT1, *SLC22A1*) [3–5], hOCT2 (*SLC22A2*) [6], and human organic anion transporters (OATP-C (*SLC21A6*) and OATP-B (*SLC21A9*)) [7].

Human H^+/peptide cotransporter 2 (hPEPT2, *SLC15A2*), expressed in a variety of tissues including the kidney, lung, and brain, mediates the uphill transport of di- and tripeptides. In addition to small peptides, hPEPT2 can transport a wide variety of peptide-like drugs such as β-lactam antibiotics and some angiotensin converting enzyme inhibitors, because these drugs are structurally similar to small peptides [8,9]. Thus, hPEPT2 works not only as a nutritional transporter but also a drug transporter. In the public SNP database NCBI dbSNP (http://www.ncbi.nlm.nih.gov/SNP/), five cSNPs with nonsynonymous changes in *hPEPT2* are reported, but functional activities of variants induced by these cSNPs have not been characterized. In the present study, we selected two cSNPs in *hPEPT2*, resulting in the amino acid changes Arg57His (R57H) and Pro409Ser (P409S), and characterized their functional activities. We demonstrated for the first time the functional impairment of hPEPT2 R57H in spite of a conserved protein expression at the cell plasma membrane.

Materials and methods

Materials. [^{14}C]Glycylsarcosine (Gly-Sar) (4.07 GBq/mmol) was obtained from Moravek Biochemicals (Brea, CA).

cDNA cloning of hPEPT2. A human kidney cDNA library, which was kindly provided by Dr. T. Abe (Tohoku University Graduate

* Corresponding author. Fax: +81-75-751-4207.
E-mail address: inui@kuhp.kyoto-u.ac.jp (K.-i. Inui).

0006-291X/$ - see front matter © 2004 Elsevier Inc. All rights reserved.
doi:10.1016/j.bbrc.2004.02.063

School of Medicine), was screened by hybridization with hPEPT2 fragments labeled with [α-^{32}P]dCTP (3000 Ci/mmol; Amersham-Pharmcia Biotech, Uppsala, Sweden) as described previously [10]. pBluescript phagemid was excised from the Uni-Zap XR vector using a helper phage and the isolated clone possessed about a 4.5 kb insert. The full-length nucleotide sequences were analyzed using a multi-capillary DNA sequencer RISA384 system (Shimadzu, Kyoto, Japan).

Construction of variants. The QuikChange site-directed mutagenesis kit (Stratagene, La Jolla, CA) was used to construct mutant cDNAs following the manufacturer's protocols using wild-type hPEPT2 cDNA inserted in the pBluescript vector as a template. The R57H (NCBI SNP ID: rs1316300) and P409S (NCBI SNP ID: rs1920305) in hPEPT2 were altered by G to A and by C to T mutations at nucleotide positions 207 and 1262, respectively (human PEPT2 reference sequence: NM_021082). The nucleotide sequences of mutants were confirmed using a multicapillary DNA sequencer RISA384 system (Shimadzu). These clones were then subcloned into the expression vector pcDNA3.1 (+) (Invitrogen, Carlsbad, CA).

Cell culture and transfection. HEK923 cells (American Type Culture Collection CRL-1573) were cultured as described previously [11,12]. pcDNA 3.1 (+) containing cDNA encoding wild-type hPEPT2 or its variants was transfected into HEK293 cells using Lipofect-AMINE 2000 Reagent (Invitrogen) according to the manufacturer's instructions. At 48 h after transfection, the cells were used for the uptake experiment and Western blot analysis.

Uptake experiment in HEK293 cells. Cellular uptake of [^{14}C]Gly-Sar was measured with monolayers grown on poly-D-lysine-coated 24-well plates. The incubation medium contained (millimolar) NaCl, 145; KCl, 3; $CaCl_2$, 1; $MgCl_2$, 0.5; D-glucose, 5, and 2-(*N*-morpholino)ethanesulfonic acid (MES), 5 (pH 6.0) or *N*-2-hydroxyethylpiperazine-*N'*-2-ethanesulfonic acid (Hepes), 5 (pH 7.4). The cells were preincubated with 0.2 mL incubation medium (pH 7.4) for 10 min at 37 °C. The medium was then removed and 0.2 mL of incubation medium (pH 6.0) containing [^{14}C]Gly-Sar was added. After 15 min incubation, the medium was aspirated, and the monolayers were rapidly washed twice with 1 mL of ice-cold incubation medium. The cells were solubilized in 0.5 mL of 0.5 N NaOH and then the radioactivity in aliquots was determined by liquid scintillation counting. The protein content of solubilized cells was determined by the method of Bradford [13] using a Bio-Rad Protein Assay Kit (Bio-Rad, Richmond, CA) with bovine γ-globulin as the standard.

Polyclonal antibody against hPEPT2. Polyclonal antibody was raised against a synthetic peptide corresponding to the intracellular domain near the COOH-terminal of hPEPT2 (KTEDMRGPADKH). The procedure for the preparation of polyclonal antibody was described previously [10].

Western blot analysis. The preparations of crude plasma membranes and procedures for Western blot analysis were also previously described [10,14]. To confirm the specificity of the antibody, the antibody was absorbed with an excess amount of antigen peptide (2 μg/ml) used as an immunogen, and Western blot analysis was carried out.

Functional expression in Xenopus oocytes. cRNA synthesis and uptake measurements were performed as described previously [14]. Indirect immunofluorescence microscopy for oocytes was performed as described [14]. Briefly, three days after injection, oocytes were fixed with 4% paraformaldehyde for 1 h, immersed in 30% sucrose for 18 h, embedded in O.C.T. compound (Sakura Finetechnical, Tokyo), and rapidly frozen at −20 °C. Sections (5 μm thick) were cut, blocked (10% goat serum), and incubated with the anti-hPEPT2 serum (1:500) for 1 h. Thereafter, sections were incubated with the Cy3 AffiniPure goat anti-rabbit IgG (H + L) at 1:100. These samples were examined with a BX-50-FLA fluorescence microscope (Olympus, Tokyo, Japan). Images were captured with a DP-50 CCD camera (Olympus) using Studio Lite software (Olympus).

Results

In the public SNP database NCBI dbSNP, five cSNPs are reported in the *SLC15A2* gene with nonsynonymous substitutions (R57H, L350F, P409S, R509K, and M704L). Recently, Leabman et al. [15] have reported that the evolutionary conservation of orthologous sequences was the best predictor of transporter function. As the sequences of human, rat, rabbit, and mouse PEPT2 were aligned, R57 and P409 were found to be conserved across the species, suggesting that alterations of these amino acids induced the functional change in hPEPT2. For other amino acid substitutions of hPEPT2, identical or similar amino acids were observed in other species. Thus, we focused on the hPEPT2 R57H and P409S variants and performed a functional characterization of them. The amino acids at positions 57 and 409 of hPEPT2 are shown in Fig. 1, which is based on the putative secondary structure model of Liu et al. [16].

First, we isolated hPEPT2 cDNA from the human kidney cDNA library. The isolated hPEPT2 cDNA was about 4.5 kb long, and the nucleotide sequence for the open reading frame was identical to that previously reported [16]. When the concentration dependence of [^{14}C]Gly-Sar uptake was examined, the K_m value of Gly-Sar was calculated at 170 μM (Fig. 2), which corresponds to reported values (74 μM) [17].

We then examined the transport activity of hPEPT2 R57H and P409S at pH 6.0. [^{14}C]Gly-Sar uptake by hPEPT2 P409S was not different from that by the wild type, whereas a complete loss of transport function of the hPEPT2 R57H variant was demonstrated (Fig. 3A). The same results were obtained in the *Xenopus* oocyte expression system (Fig. 3B).

To examine whether expression of hPEPT2 R57H is altered in HEK293 cells, Western blot analysis was performed. As shown in Fig. 4A, an immunoreactive protein with a molecular weight of about 90 kDa was detected in the cells transfected with wild-type hPEPT2 and its variants, but not vector alone. The expression

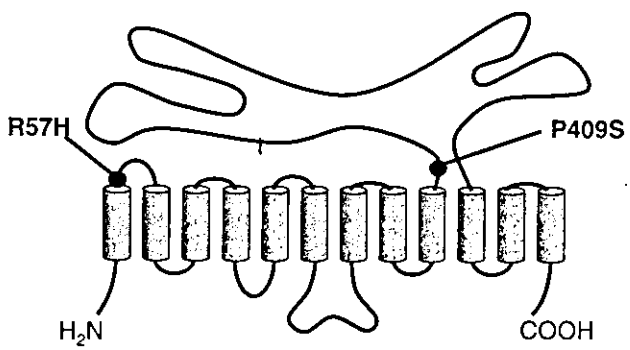

Fig. 1. hPEPT2 protein topology and the positions of the analyzed cSNP resulting in R57H and P409S.

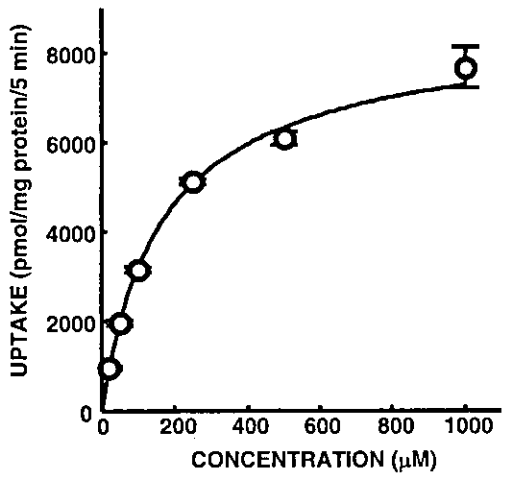

Fig. 2. Concentration dependence of [^{14}C]Gly-Sar uptake by HEK293 cells transiently expressing wild-type hPEPT2. HEK293 cells transfected with wild-type hPEPT2 were incubated with various concentrations of [^{14}C]Gly-Sar (pH 6.0) for 5 min at 37 °C. Each point represents the mean ± SE for three monolayers.

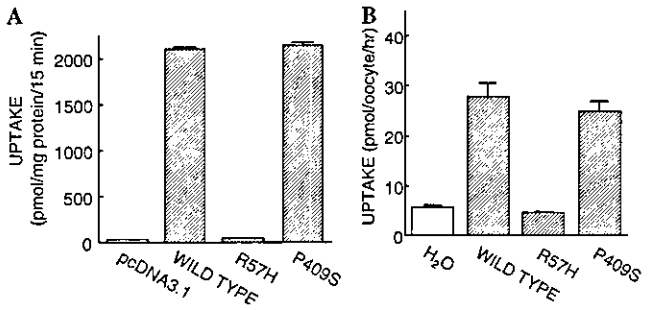

Fig. 3. [^{14}C]Gly-Sar uptake by HEK293 cells (A) and by oocytes (B) transiently expressing wild-type hPEPT2 and its variants R57H and P409S. (A) HEK293 cells transfected with vector alone (pcDNA3.1), wild-type hPEPT2 (wild type) and its variant (R57H and P409S) cDNA, were incubated with 20 μM [^{14}C]Gly-Sar (pH 6.0) for 15 min at 37 °C. Each column represents the mean ± SE for three monolayers. (B) Oocytes injected with H_2O, wild-type hPEPT2 and its variant (R57H and P409S) cRNA were incubated with 20 μM [^{14}C]Gly-Sar for 1 h at 25 °C. Each column represents the mean ± SE for 8 oocytes.

levels are comparable among the wild type and two variants. These positive bands disappeared when the antiserum was preabsorbed with the hPEPT2 antigen peptide (Fig. 4B). Furthermore, as shown in Fig. 5, the hPEPT2 R57H variant protein was expressed at plasma membranes as well as the wild type and P409S variant in the *Xenopus* oocyte expression system. These findings suggested that the loss of transport function of the hPEPT2 R57H variant was not due to a change in membrane protein expression.

The loss of transport function of hPEPT2 R57H may be caused by the differences in the charge of the side chain of arginine and histidine. The ratio of the non-protonated (neutral) to protonated (positive) side chain of arginine (side chain $pK_a = 12.5$) is 1:3,160,000 at pH 6.0, whereas that of histidine (side chain $pK_a = 6.0$) is

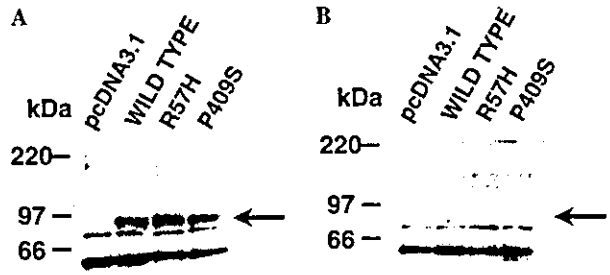

Fig. 4. Western blot analysis of crude membranes obtained from HEK293 cells transiently expressing with wild-type hPEPT2 and its variants R57H and P409S. Crude membranes (20 μg) obtained from HEK293 cells transiently transfected with vector alone (pcDNA3.1), wild-type hPEPT2 (wild type) and its variant (R57H and P409S) cDNAs were separated by SDS–PAGE (8.5%) and blotted onto PVDF membranes. The antiserum for hPEPT2 (1:500) was used as primary antibody without (A) or with (B) the antigen peptide (2 μg/ml) of hPEPT2. A horseradish peroxidase-conjugated anti-rabbit IgG antibody was used for detection of bound antibodies, and the strips of blots were visualized by chemiluminescence on X-ray film. The arrowhead indicates the position of hPEPT2.

1:1. Thus, we next measured the [^{14}C]Gly-Sar uptake at various pHs by the hPEPT2 wild type and two variants. As shown in Fig. 6, at all pH values tested, [^{14}C]Gly-Sar uptake by the wild type and P409S variant was comparable, whereas the transport activity of hPEPT2 R57H was completely lost.

Discussion

To date, there has been no report concerning the functional characterization of cSNPs of *SLC15A* genes. Here, we have demonstrated for the first time that an amino acid substitution (R57H) of hPEPT2 due to a cSNP caused a complete loss of transport function. According to recent studies in *Pept2* knockout mice, *Pept2*$^{-/-}$ mice were healthy and fertile, but dipeptide transport in the choroid plexus and kidney was reduced [18,19]. In addition to small peptides, Ocheltree et al. [20] have recently demonstrated that the uptake of cefadroxil, an oral β-lactam antibiotic, in the choroid plexus was reduced by 83% in *Pept2*$^{-/-}$ mice as compared to *Pept2*$^{+/+}$ mice, and suggested that PEPT2 is the primary transporter responsible for the choroid plexus uptake of peptide-like drugs at the blood–cerebrospinal fluid–barrier. If the findings in knockout mice can be extrapolated to humans, the homozygotes for this allele are healthy, but the handling of small peptides and peptide-like drugs in the choroid plexus and kidney may

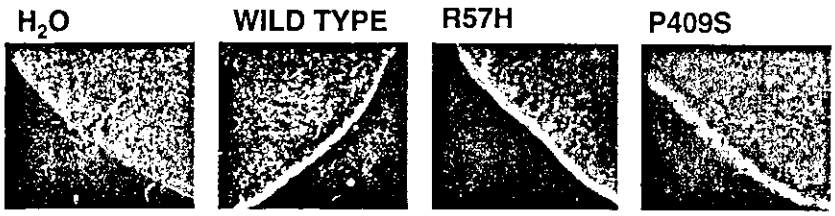

Fig. 5. Expression of wild-type hPEPT2 and its variant R57H and P409S in *Xenopus* oocytes. *Xenopus* oocytes injected with H_2O, wild-type hPEPT2 (wild type) and its variants (R57H and P409S) cRNAs were fixed and stained with antiserum for hPEPT2. Cy3-labeled anti-rabbit IgG was used for detection of bound antibodies.

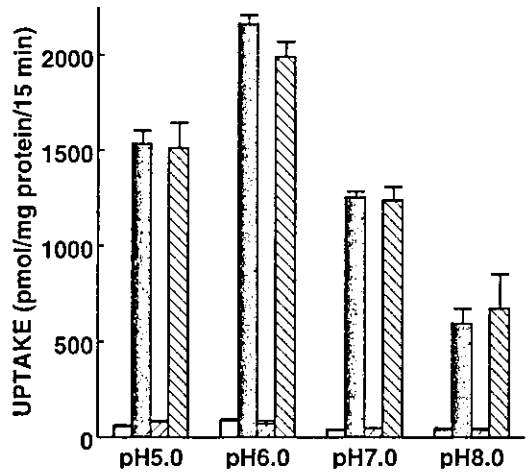

Fig. 6. pH-dependence of [^{14}C]Gly-Sar uptake by HEK293 cells transiently expressing wild-type hPEPT2 and its variants R57H and P409S. HEK293 cells transfected with vector alone (□), wild-type hPEPT2 (■), R57H (▨), and P409S (▧) cDNAs were incubated with 20 μM [^{14}C]Gly-Sar at various pHs for 15 min at 37 °C. Each column represents the mean ± SE for three monolayers.

be affected. Further clinical studies are needed to see whether this SNP affects the pharmacokinetic profiles of peptide-like drugs and might be responsible for inter-individual differences during drug therapy.

The present findings also provided significant information on the biology of H^+/peptide cotransporters. Interestingly, the critical amino acid residue Arg57 we identified is conserved in PEPT1 and PEPT2 across human, rat, rabbit, and mouse. Furthermore, recent functional analyses of chimeric PEPT1/PEPT2 proteins demonstrated that the N-terminal regions up to the second transmembrane domain (TMD) may form an important part of the peptide transporters [21]. As Arg57 is included in this region (Fig. 1), our data support the functional importance of this domain. What is the role of Arg residue at position 57 in hPEPT2? There have been several reports on the functional roles of the Arg residue in different transporters [22–24]. For example, in the lactose/H^+ symporter, Arg302 of this transporter facilitated the deprotonation of the carboxylic acid of Glu325 during the H^+ translocation process [23]. In the present study, we found that the R57H variant did not show transport activity at pH 5.0–8.0. It is noted that, at pH 5.0, the ratio of non-protonated to protonated side chain of histidine is 1:10, suggesting that the positive charge of the amino acid at position 57 did not compensate for the transport activity. Further studies are needed to determine the functional roles of Arg57 of hPEPT2.

Using site-directed mutagenesis, conserved His residues in the second and fourth TMDs of PEPT1 and PEPT2 were shown to be essential for the transport activity and/or substrate binding [14,25–27]. One His residue was suggested to be the binding site for the α-amino group of substrates [28] and the other a H^+-binding site [14,25–27]. Thus, there is the possibility that the loss of transport function in the R57H variant may be caused by interference of the His residue at position 57 by His residues located in the second and fourth TMDs of hPEPT2.

In conclusion, we demonstrated that the hPEPT2 R57H variant induced by cSNP G207A showed no transport activity in spite of a normal expression at the plasma membranes. These findings suggest that both peptide homeostasis and pharmacokinetic profiles of peptide-like drugs may be altered in homozygotes for this variant.

Acknowledgments

This work was supported by the 21st Century COE Program "Knowledge Information Infrastructure for Genome Science," a Grant-in-Aid for Comprehensive Research on Aging and Health from the Ministry of Health, Labor and Welfare of Japan, and a Grant-in-Aid for Scientific Research from the Ministry of Education, Culture, Sports, Science and Technology of Japan. This work was carried out in collaboration with a PharmaSNP consortium.

References

[1] W.E. Evans, M.V. Relling, Pharmacogenomics: translating functional genomics into rational therapeutics, Science 286 (1999) 487–491.

[2] W.E. Evans, H.L. McLeod, Pharmacogenomics—drug disposition, drug targets, and side effects, N. Engl. J. Med. 348 (2003) 538–549.

[3] R. Kerb, U. Brinkmann, N. Chatskaia, D. Gorbunov, V. Gorboulev, E. Mornhinweg, A. Keil, M. Eichelbaum, H. Koepsell, Identification of genetic variations of the human organic

cation transporter hOCT1 and their functional consequences, Pharmacogenetics 12 (2002) 591–595.
[4] Y. Shu, M.K. Leabman, B. Feng, L.M. Mangravite, C.C. Huang, D. Stryke, M. Kawamoto, S.J. Johns, J. DeYoung, E. Carlson, T.E. Ferrin, I. Herskowitz, K.M. Giacomini, Evolutionary conservation predicts function of variants of the human organic cation transporter, OCT1, Proc. Natl. Acad. Sci. USA 100 (2003) 5902–5907.
[5] A. Takeuchi, H. Motohashi, M. Okuda, K. Inui, Decreased function of genetic variants, Pro283Leu and Arg287Gly, in human organic cation transporter *hOCT1*, Drug Metab. Pharmacokinet. 18 (2003) 409–412.
[6] M.K. Leabman, C.C. Huang, M. Kawamoto, S.J. Johns, D. Stryke, T.E. Ferrin, J. DeYoung, T. Taylor, A.G. Clark, I. Herskowitz, K.M. Giacomini, Polymorphisms in a human kidney xenobiotic transporter, OCT2, exhibit altered function, Pharmacogenetics 12 (2002) 395–405.
[7] T. Nozawa, M. Nakajima, I. Tamai, K. Noda, J. Nezu, Y. Sai, A. Tsuji, T. Yokoi, Genetic polymorphisms of human organic anion transporters OATP-C (SLC21A6) and OATP-B (SLC21A9): allele frequencies in the Japanese population and functional analysis, J. Pharmacol. Exp. Ther. 302 (2002) 804–813.
[8] H. Daniel, I. Rubio-Aliaga, An update on renal peptide transporters, Am. J. Physiol. Renal Physiol. 284 (2003) F885–F892.
[9] K. Inui, T. Terada, Dipeptide transporters, in: G.L. Amidon, W. Sadée (Eds.), Membrane Transporters as Drug Targets, Kluwer Academic/Plenum Publishers, New York, 1999, pp. 269–288.
[10] H. Saito, M. Okuda, T. Terada, S. Sasaki, K. Inui, Cloning and characterization of a rat H^+/peptide cotransporter mediating absorption of β-lactam antibiotics in the intestine and kidney, J. Pharmacol. Exp. Ther. 275 (1995) 1631–1637.
[11] Y. Urakami, M. Akazawa, H. Saito, M. Okuda, K. Inui, cDNA cloning, functional characterization, and tissue distribution of an alternatively spliced variant of organic cation transporter hOCT2 predominantly expressed in the human kidney, J. Am. Soc. Nephrol. 13 (2002) 1703–1710.
[12] N. Horiba, S. Masuda, C. Ohnishi, D. Takeuchi, M. Okuda, K. Inui, Na^+-dependent fructose transport via rNaGLT1 in rat kidney, FEBS Lett. 546 (2003) 276–280.
[13] M.M. Bradford, A rapid and sensitive method for the quantitation of microgram quantities of protein utilizing the principle of protein-dye binding, Anal. Biochem. 72 (1976) 248–254.
[14] T. Terada, H. Saito, M. Mukai, K. Inui, Identification of the histidine residues involved in substrate recognition by a rat H^+/peptide cotransporter, PEPT1, FEBS Lett. 394 (1996) 196–200.
[15] M.K. Leabman, C.C. Huang, J. DeYoung, E.J. Carlson, T.R. Taylor, M. de la Cruz, S.J. Johns, D. Stryke, M. Kawamoto, T.J. Urban, D.L. Kroetz, T.E. Ferrin, A.G. Clark, N. Risch, I. Herskowitz, K.M. Giacomini, Natural variation in human membrane transporter genes reveals evolutionary and functional constraints, Proc. Natl. Acad. Sci. USA 100 (2003) 5896–5901.
[16] W. Liu, R. Liang, S. Ramamoorthy, Y.J. Fei, M.E. Ganapathy, M.A. Hediger, V. Ganapathy, F.H. Leibach, Molecular cloning of PEPT 2, a new member of the H^+/peptide cotransporter family, from human kidney, Biochim. Biophys. Acta 1235 (1995) 461–466.
[17] S. Ramamoorthy, W. Liu, Y.Y. Ma, T.L. Yang-Feng, V. Ganapathy, F.H. Leibach, Proton/peptide cotransporter (PEPT 2) from human kidney: functional characterization and chromosomal localization, Biochim. Biophys. Acta 1240 (1995) 1–4.
[18] H. Shen, D.E. Smith, R.F. Keep, J. Xiang, F.C. Brosius III, Targeted disruption of the PEPT2 gene markedly reduces dipeptide uptake in choroid plexus, J. Biol. Chem. 278 (2003) 4786–4791.
[19] I. Rubio-Aliaga, I. Frey, M. Boll, D.A. Groneberg, H.M. Eichinger, R. Balling, H. Daniel, Targeted disruption of the peptide transporter Pept2 gene in mice defines its physiological role in the kidney, Mol. Cell. Biol. 23 (2003) 3247–3252.
[20] S.M. Ocheltree, H. Shen, Y. Hu, J. Xiang, R.F. Keep, D.E. Smith, Mechanisms of cefadroxil uptake in the choroid plexus: studies in wild type and PEPT2 knockout mice, J. Pharmacol. Exp. Ther. 308 (2004) 462–467.
[21] F. Doring, C. Martini, J. Walter, H. Daniel, Importance of a small N-terminal region in mammalian peptide transporters for substrate affinity and function, J. Membr. Biol. 186 (2002) 55–62.
[22] X. Yao, A.M. Pajor, Arginine-349 and aspartate-373 of the Na^+/dicarboxylate cotransporter are conformationally sensitive residues, Biochemistry 41 (2002) 1083–1090.
[23] M. Sahin-Toth, H.R. Kaback, Arg-302 facilitates deprotonation of Glu-325 in the transport mechanism of the lactose permease from *Escherichia coli*, Proc. Natl. Acad. Sci. USA 98 (2001) 6068–6073.
[24] A. Bendahan, A. Armon, N. Madani, M.P. Kavanaugh, B.I. Kanner, Arginine 447 plays a pivotal role in substrate interactions in a neuronal glutamate transporter, J. Biol. Chem. 275 (2000) 37436–37442.
[25] Y.J. Fei, W. Liu, P.D. Prasad, R. Kekuda, T.G. Oblak, V. Ganapathy, F.H. Leibach, Identification of the histidyl residue obligatory for the catalytic activity of the human H^+/peptide cotransporters PEPT1 and PEPT2, Biochemistry 36 (1997) 452–460.
[26] X.Z. Chen, A. Steel, M.A. Hediger, Functional roles of histidine and tyrosine residues in the H^+-peptide transporter PepT1, Biochem. Biophys. Res. Commun. 272 (2000) 726–730.
[27] T. Uchiyama, A.K. Kulkarni, D.L. Davies, V.H.L. Lee, Biophysical evidence fro His^{57} as a proton-binding site in the mammalian intestinal transporter hPepT1, Pharm. Res. 20 (2003) 1911–1916.
[28] T. Terada, H. Saito, K. Inui, Interaction of β-lactam antibiotics with histidine residue of rat H^+/peptide cotransporters, PEPT1 and PEPT2, J. Biol. Chem. 273 (1998) 5582–5585.

J Hum Genet (2004) 49:40–45
DOI 10.1007/s10038-003-0105-4

ORIGINAL ARTICLE

Yuichi Uwai · Satohiro Masuda · Maki Goto
Hideyuki Motohashi · Hideyuki Saito
Masahiro Okuda · Eijirou Nakamura · Noriyuki Ito
Osamu Ogawa · Ken-ichi Inui

Common single nucleotide polymorphisms of the *MDR1* gene have no influence on its mRNA expression level of normal kidney cortex and renal cell carcinoma in Japanese nephrectomized patients

Received: 28 July 2003 / Accepted: 28 October 2003 / Published online: 18 December 2003
© The Japan Society of Human Genetics and Springer-Verlag 2003

Abstract In this study, we have quantified the mRNA expression levels of multidrug resistance gene 1 (MDR1) in the normal kidney cortex and renal cell carcinoma (RCC) segments from 24 Japanese nephrectomized patients by real-time polymerase chain reaction (PCR). The mRNA expression level of MDR1 in RCC segments was significantly decreased in comparison with each normal segment ($P=0.0042$, by Student's paired t-test). In addition, the ten common single nucleotide polymorphisms (SNPs) of the *MDR1* gene in the patients were assessed using the PCR-restriction enzyme fragment length polymorphism method to investigate the influence of these SNPs on its mRNA expression levels. The allele frequencies of these SNPs were comparable with our previous report in the Japanese recipients of living-donor liver transplantation (Goto et al., Pharmacogenetics 12:451–457; 2002). MDR1 expression levels in the normal kidney cortex were independent on the five SNPs, which were polymorphic in the Japanese population. Furthermore, the effect of the SNPs on expression levels of MDR1 mRNA in RCC segments was not recognized. These findings suggest that the common SNPs in the *MDR1* gene have no influence on the expression of its transcript in RCC segments as well as in the normal kidney cortex.

Keywords MDR1 · SNP · Kidney · Renal cell carcinoma

Y. Uwai · S. Masuda · M. Goto · H. Motohashi · H. Saito
M. Okuda · K. Inui (✉)
Department of Pharmacy, Kyoto University Hospital,
Sakyo-ku, Kyoto 606-8507, Japan
E-mail: inui@kuhp.kyoto-u.ac.jp
Tel.: +81-75-7513577
Fax: +81-75-7514207

E. Nakamura · N. Ito · O. Ogawa
Department of Urology, Graduate School of Medicine,
Kyoto University, Kyoto, Japan

Introduction

An ATP-driven efflux pump P-glycoprotein (Pgp), the multidrug resistance 1 (*MDR1* or *ABCB1*) gene product, is expressed in the plasma membrane of several tumor and normal cells and mediates extrusion of endogenous compounds, xenobiotics and drugs including anticancer drugs, cardiac glycosides, immunosuppressants, and anthracycline antibiotics (Ambudkar et al. 1999). Besides Pgp one of component molecules for the multidrug resistance of tumor cells, the transporter is now accepted as playing an important role for intestinal absorption, tissue distribution, and biliary or urinary excretion of drugs in normal tissues (Ambudkar et al. 1999).

Single nucleotide polymorphisms (SNPs) exist in the *MDR1* gene, and the relationship between SNPs and the expression/function of MDR1 has been reported by several laboratories. First, Hoffmeyer et al. (2000) represented that the C3435T SNP in the *MDR1* gene influenced the expression level of Pgp in the duodenum and that the absorption rate of orally administered digoxin was dependent on the SNP in healthy Caucasians. However, following examinations comparing SNPs in the *MDR1* gene with drug absorption and/or the intestinal expression level of Pgp, MDR1 have not been reproducible (Kim et al. 2001; Kurata et al. 2002; Goto et al. 2002; Gerloff et al. 2002). Recently, Siegsmund et al. (2002) demonstrated that the allele T of cDNA 3435 in the *MDR1* gene reduced Pgp expression in the kidney. However, there are few reports illustrating in detail the renal MDR1 expression with influences by its genetic variations.

Renal malignant tumors account for more than 2% of cancer incidence, and renal cell carcinoma (RCC) compose the majority in renal tumors. RCC shows resistance against chemotherapy (Hartmann and Bokemeyer 1999), and it is suggested that Pgp is involved in the chemoresistance of RCC (Fojo et al. 1987; Kakehi et al. 1988). Siegsmund et al. (2002) also suggested that

the C3435T SNP in the *MDR1* gene would be a risk factor for the development of RCC in Caucasians. In spite of suggesting the significance of Pgp and/or *MDR1* SNPs on the patients with RCC described above, the role of Pgp for chemoresistance of RCC has remained to be elucidated.

In the present study, we quantified the mRNA levels of MDR1 in the normal kidney cortex and RCC segments from Japanese nephrectomized patients with renal tumors. In addition, the ten common SNPs of the *MDR1* gene in these patients were examined, and the association between genotypes and expression level was assessed.

Materials and methods

Patients

Twenty-four Japanese patients who were surgically nephrectomized with RCC at Kyoto University Hospital were enrolled in this study. The subjects consisted of 18 men and six women whose ages ranged from 39 to 74 (63.6± 8.5, mean ± SD) years. The nephrectomized segments of the normal cortex and RCC were obtained after receiving written informed consent. The study was performed in accordance with the Declaration of Helsinki and its amendments, and was approved by the Ethics Committee of Kyoto University Graduate School and Faculty of Medicine.

Isolation of total RNA and genomic DNA

Total RNA and genomic DNA from a renal homogenate in a guanidinium thiocyanate solution were isolated with a MagNA Pure LC RNA isolation kit II and DNA isolation kit (Roche Diagnostic GmbH, Mannheim, Germany), respectively, as previously described (Goto et al. 2002; Motohashi et al. 2002). The isolated total RNA was reverse-transcribed, and the single stranded DNA was used for quantification of MDR1 mRNA levels. Genotyping of the *MDR1* gene was performed using genomic DNA.

Quantification of MDR1 mRNA expression levels

MDR1 mRNA levels in the normal kidney cortex and RCC segments were measured by real-time polymerase chain reaction (PCR), as previously described (Motohashi et al. 2002). The primer/probe set for the specific amplification of MDR1 was designed according to parameters incorporated in the Primer Express software (PE Biosystems, Foster City, CA, USA). The forward and reverse primers were GCTCAGACAGGATGTGAGTTGGT (position; 2812–2834, accession number M14758 in GenBank database) and CCTGGAACCTATAGCCCCTTTAAC (position; 2897–2920), respectively. The sequence of TaqMan probe was AAAAACACCACTGGAGCATTGACTACCAGG, corresponding to the position 2846–2875. Real-time PCR was performed in a total volume of 20 µl containing 2 µl of reverse-transcribed cDNA, 1 µM forward and reverse primers, 0.2 µM TaqMan probe, and 10 µl TaqMan Universal PCR Master Mix (Applied Biosystems, Foster City, CA, USA). The PCR condition was as follows: 50 cycles of 94°C for 15 s and 60°C for 60 s. The copy number of the target mRNA sequence in the starting materials was established by determining the fractional PCR threshold cycle number (Ct) at which a fluorescence signal generated during the replication process passed above a threshold value. The initial amount of target mRNA in each sample was estimated from the Ct value with a standard curve generated using known amounts of standard plasmid DNA. Glyceraldehyde-3-phosphate dehydrogenase mRNA was also quantified as an internal control with glyceraldehyde-3-phosphate dehydrogenase control reagent (Applied Biosystems).

Genotyping of the *MDR1* gene

The genotype of the *MDR1* gene was investigated by PCR-restriction enzyme fragment length polymorphism methods. The specific primers and restriction enzymes used in this study were as previously described (Goto et al. 2002). The PCR conditions were as follows: after denaturing at 94°C for 3 min, the PCR was performed with 1 µM of each primer and Taq DNA polymerase (Takara, Shiga, Japan), according to the following profile: 94°C for 30 s, 60°C for 30 s, and 72°C for 30 s, 35 cycles, following by a single additional 10-min extension at 72°C. The PCR products were digested with or without restriction enzymes and separated on 3.5% agarose gel.

Statistical analysis

The difference in the logarithmically transformed data of MDR1 mRNA expressions between normal cortex and RCC was analyzed using Student's paired *t*-test. The correlation between the *MDR1* genotype and its mRNA expression was analyzed using the Mann-Whitney *U* test. *P* values < 0.05 were considered to be significant.

Results

Quantification of MDR1 mRNA in normal kidney cortex and renal cell carcinoma

Figure 1 shows distribution histograms of logarithmically transformed mRNA levels of MDR1 in the normal kidney cortex and RCC segments. The average mRNA expression levels of MDR1 in the normal kidney cortex and RCC segments were 19.0 and 6.6 amol/µg total RNA, respectively. A statistical significant difference of the MDR1 mRNA levels in normal kidney cortex and RCC segments of each patient was observed ($P = 0.0042$, Fig. 2).

Genotype frequency of ten common SNPs of the *MDR1* gene in nephrectomized patients

The genotype of the *MDR1* gene from the normal kidney cortex and RCC segments was assessed at ten common nucleotide positions in 24 Japanese patients. No differences in *MDR1* genotypes from both segments of each patient were found. Frequencies of the genetic variants are summarized in Table 1. In this study, variants at exon 2–1, cDNA 61, cDNA 307, cDNA 1199, and exon 12+44 were not observed. A variant leading to amino acid exchange was observed only at cDNA 2677. The allele frequency of the cDNA 2677 was 45.8% for allele T and 18.8% for allele A. At cDNA 1236 and 3435, which do not influence amino acid substitute, genetic variants were recognized. Allele frequencies were 66.7% for allele T at cDNA 1236 and 52.1% for allele T at cDNA 3435. A complete linkage was observed

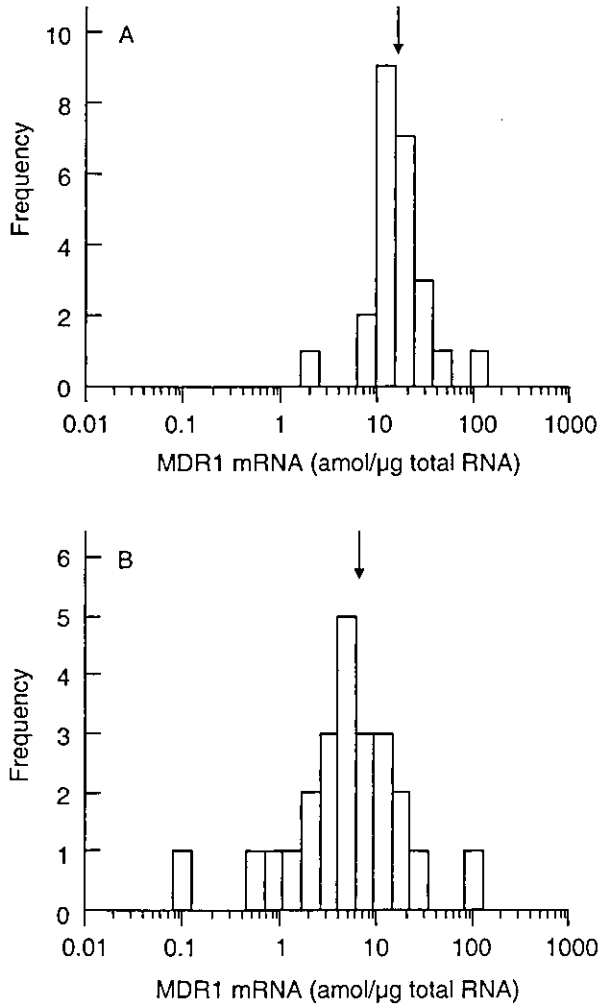

Fig. 1A, B Distribution histograms of MDR1 mRNA expression levels in normal kidney cortex (A) and renal cell carcinoma (B). MDR1 mRNA levels were logarithmically transformed to improve normality. The *arrows* indicate the mean values of MDR1 mRNA expression levels

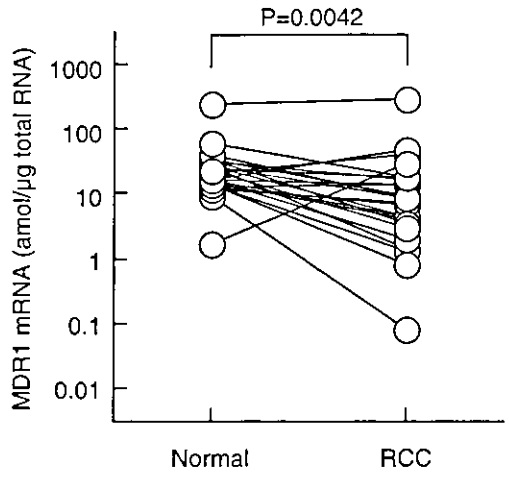

Fig. 2 Effect of malignant transformation on renal MDR1 mRNA levels in 24 patients with renal cell carcinoma

between cDNA 1236 C/T and an intronic variant of exon 6+139 C/T. Another intronic variant at exon 17–76 was determined with the frequency of 31.3% for allele A. These allele frequencies were comparable with our previous reports in Japanese recipients of living-donor liver transplantation.

Correlation between *MDR1* SNPs and MDR1 mRNA expression in normal kidney cortex and renal cell carcinoma

Next, we examined the association between the *MDR1* gene and its mRNA levels in the normal kidney cortex and RCC. As shown in Fig. 3, the significant effects of each SNP on MDR1 mRNA expression in the normal kidney cortex and RCC segments were not recognized. However, the MDR1 mRNA levels in the kidney were significantly reduced by transformation to RCC with C/T of cDNA 1236 and exon 6+139, T/A and T/T of exon 17–76, G/T of cDNA 2677, and C/T at cDNA 3435.

Discussion

In the present study, MDR1 mRNA levels in the human kidney cortex were quantified using the real-time PCR method. We previously examined its mRNA expression levels in the small intestine in Japanese recipients of living-donor liver transplantation. The MDR1 mRNA levels in the kidney cortex were about 40-fold higher than those in the intestinal mucosa (Goto et al. 2002; Hashida et al. 2001). Even if the mucosal samples derived from patients in end-stage liver failure were considered, the MDR1 mRNA contents in the kidney cortex were markedly higher compared to the intestine. To our knowledge, this is the first study of the quantification of MDR1 mRNA level in the human kidney cortex.

It is generally accepted that the majority of administered digoxin, a cardiac glycoside, is excreted into urine and that Pgp plays an important role for its tubular secretion (Tanigawara et al. 1992). In addition, concomitant administration with various drugs, including cyclosporin A, calcium channel blockers, macrolide antibiotics, and azole antifungal drugs elevates serum concentration of digoxin, at least in part, via renal tubular Pgp (Rodin and Johnson 1988; Wakasugi et al. 1998). Considering these pharmacokinetic significances of renal Pgp, the expression levels and activity of Pgp in the kidney would be a key factor for the optimal dosage regimen of digoxin.

The present findings represent a wide interindividual variation of MDR1 mRNA levels in the human kidney cortex (about 140-fold), and no relationship between the ten common SNPs of the *MDR1* gene and its mRNA expression levels. It was reported that the interindividual variation of MDR1 expression also existed in the human small intestine and liver, suggesting that expression variation has been responsible for interindividual

Table 1 *MDR1* genetic variants in 24 Japanese nephrectomized patients

Location	Position	Allele	Effect	Frequency	Genotype	Frequency	Goto et al.[a]
Intron 1	Exon 2–1	G	Initiation of translation?	100	G/G	100	100
		A		0	G/A	0	0
					A/A	0	0
Exon 2	cDNA 61	A	21 Asn	100	A/A	100	100
		G	21 Asp	0	A/G	0	0
					G/G	0	0
Exon 5	cDNA 307	T	103 Phe	100	T/T	100	100
		C	103 Leu	0	T/C	0	0
					C/C	0	0
Intron 6	Exon 6+139	C	?	33.3	C/C	8.3	10.3
		T		66.7	C/T	50	52.9
					T/T	41.7	36.8
Exon 11	cDNA 1199	G	400 Ser	100	G/G	100	100
		A	400 Asn	0	G/A	0	0
					A/A	0	0
Exon 12	cDNA 1236	C	Wobble	33.3	C/C	8.3	10.1
		T		66.7	C/T	50	49.3
					T/T	41.7	40.6
Intron 12	Exon 12+44	C	?	100	C/C	100	100
		T		0	C/T	0	0
					T/T	0	0
Intron 16	Exon 17–76	T	?	68.8	T/T	45.8	42.6
		A		31.3	T/A	45.8	51.5
					A/A	8.3	5.9
Exon 21	cDNA 2677	G	893 Ala	35.4	G/G	0	22.9
		T	893 Ser	45.8	G/A	29.2	5.8
		A	893 Thr	18.8	G/T	41.7	39.1
					T/A	8.3	15.9
					T/T	20.8	15.9
					A/A	0	1.4
Exon 26	cDNA 3435	C	Wobble	47.9	C/C	25	30.4
		T		52.1	C/T	45.8	50.7
					T/T	29.2	18.8

[a]These values are from our previous study with Japanese recipients of living-donor liver transplantation

variation of drug absorption and disposition (Goto et al. 2002; Hashida et al. 2001; Schuetz et al. 1995). A nuclear receptor, pregnane X receptor (termed as steroid and xenobiotic receptor), predominantly expressed in the liver and small intestine, was reported to regulate MDR1 expression in these tissues as a part of the regulatory mechanisms by various compounds including endogenous steroids and xenobiotics (Synold et al. 2001). Therefore, the nuclear receptor may contribute, at least in part, to the large interindividual variability of the expression level of MDR1 in the liver and small intestine. However, there is no information predicting the expression regulation of renal Pgp. The elucidation of the nuclear receptors and SNPs in the transcriptional regulatory region of the *MDR1* gene would clarify interindividual variation of renal Pgp content.

During the last few decades, the incidence of RCC has steadily increased (Chow et al. 1999). Obesity, hypertension, gender, smoking, and several drugs such as diuretics, phenacetin, and aspirin are suggested to be associated with RCC (Dhote et al. 2000). Furthermore, various genetic polymorphisms were also reported to be related to the disease (Nakamura et al. 2002; Tanaka et al. 2002). Recently, Siegsmund et al. (2002) reported that the frequency of T/T genotype at MDR1 cDNA 3435 was significantly higher in patients with RCC than in the control Caucasians, suggesting that this SNP would be a risk factor for RCC in Caucasian. In this study, the T/T was observed in seven of 24 RCC patients (29.2%). Since this frequency is not significantly different from healthy Japanese (20%) in the data reported by Schaeffeler et al.(2001) with χ^2 statistics ($P > 0.540$), the T/T genotype at MDR1 cDNA 3435 might not be a risk factor for RCC in Japanese. Further research is needed to elucidate the association between the cDNA 3435 SNP and RCC in Japanese. Chow et al. (1999) reported the incidence of RCC in black subjects was higher than in Caucasian subjects. On the other hand, the frequency of the T/T genotype at the cDNA 3435 is reported to be markedly lower in black subjects than in Caucasian and Japanese subjects (Schaeffeler et al. 2001). The T/T frequency in black subjects with RCC should be interested. Siegsmund et al. (2002) also represented that Pgp expression levels in renal noncancerous segments were significantly lower with the T/T genotype at cDNA 3435 than with the C/C genotype by using the quantitative immunohistochemistry method. This suggests that renal Pgp expression levels influence susceptibility to the development of renal epithelial cancers. Our work illustrates that MDR1 levels were not affected by the cDNA 3435 T/T genotype. In the future, not only to determine the predominant factor(s)/material(s) developing RCC but also to clarify its renal handling, including the contribution of Pgp, are necessary for

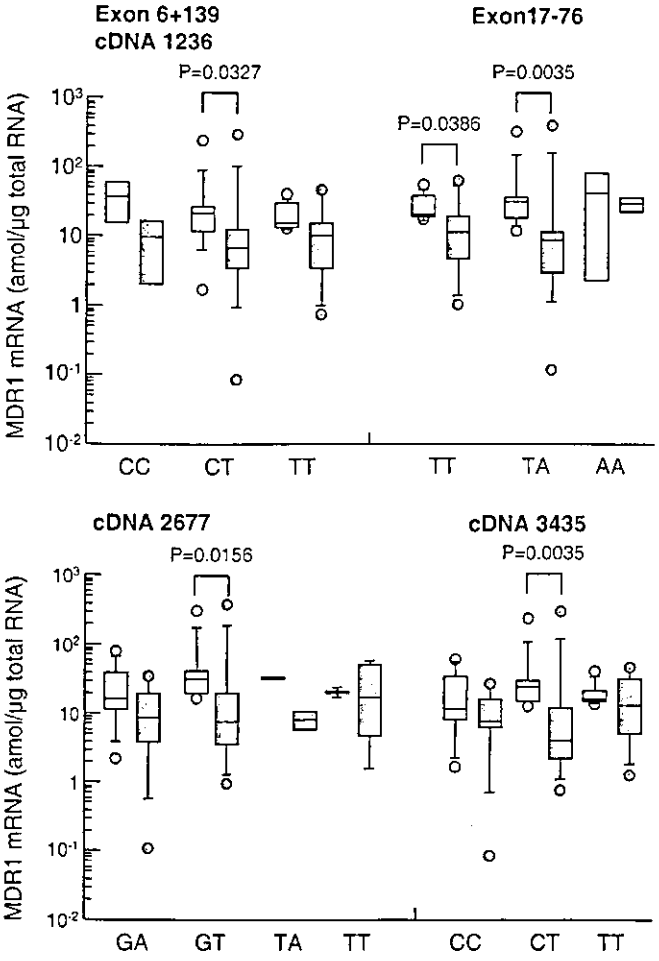

Fig. 3 Comparison of mRNA levels in the normal kidney cortex, renal cell carcinoma (RCC) segments, or their variation by carcinogenesis with the *MDR1* genotype. The MDR1 mRNA levels in the normal kidney cortex (*open box*) and RCC segments (*gray box*) were compared with the five polymorphic SNPs. Simultaneously, the variation of the expression levels of MDR1 mRNA were assessed in comparison with the *MDR1* genotypes between normal and RCC segments. After statistical analyses by Mann-Whitney *U* test, *P* values less than 0.05 were shown

analysis of the relationship between RCC and the SNP of the *MDR1* gene.

RCC displays an intrinsically high degree of resistance to chemotherapy (Hartmann and Bokemeyer 1999). Fojo et al. (1987) and Kakehi et al. (1988) represented that the resistance of RCC against anticancer drug vinblastine was associated with MDR1 expression using cell lines. The present study clarified that MDR1 expression levels showed a downward tendency by malignant transformation to RCC and that expression in the RCC was still relatively high. These results are compatible with other groups (Fojo et al. 1987; Kakehi et al. 1988). Taken together with the fact that various anticancer drugs are substrates of Pgp, it is suggested that this phenomenon is, at least in part, involved in the chemoresistance of RCC. The downregulation of MDR1 mRNA in the kidney cortex by transformation to RCC was dependent on the T allele at exon 17–76 (Fig. 3). Despite the small number of patients carrying the A/A genotype at exon 17–76 ($n=2$), the mRNA expression of MDR1 in the kidney might be downregulated by carcinogenesis in patients with the T allele. Therefore, further studies would clarify the effect of SNPs in the *MDR1* gene on the reducing rate of its mRNA level in renal tissue by carcinogenesis. In addition to MDR1, glutathione S-transferase, topoisomerase II, and MDR-associated protein are suggested to contribute to the chemoresistance of RCC (Volm et al. 1993; Kim et al. 1996). Elucidation of not only renal handling of anticancer agents but also function and expression levels of these proteins in RCC, and of their relations with SNPs, give information for the adequate selection of anticancer agents for individual RCC.

In summary, we estimated the copy number of MDR1 mRNA in the human kidney cortex and RCC and found that there is a wide interindividual variation in renal MDR1 expression levels and that MDR1 mRNA levels tend to decrease by malignant transformation to RCC in the human kidney. In addition, the ten common polymorphisms of the *MDR1* gene were examined, and the effect of SNPs on expression levels of the transporter mRNA was not observed in the normal kidney cortex and RCC. To our knowledge, this is the first report representing the measurement of renal MDR1 mRNA and correlation of the expression and SNPs of *MDR1*.

Acknowledgements This work was supported by a grant-in-aid for Research on Human Genome, Tissue Engineering, and Food Biotechnology from the Ministry of Health, Labor, and Welfare of Japan (H12-Genome-019), a grant-in-aid for Scientific Research from the Ministry of Education, Culture, Sports, Science, and Technology of Japan, and the 21st Century COE Program "Knowledge Information Infrastructure for Genome Science". M.G. is supported as a Research Assistant by the 21st Century COE Program "Knowledge Information Infrastructure for Genome Science".

References

Ambudkar SV, Dey S, Hrycyna CA, Ramachandra M, Pastan I, Gottesman MM (1999) Biochemical, cellular, and pharmacological aspects of the multidrug transporter. Annu Rev Pharmacol Toxicol 39:361–398

Chow WH, Devesa SS, Warren JL, Fraumeni, JF Jr (1999) Rising incidence of renal cell cancer in the United States. JAMA 281:1628–1631

Dhote R, Pellicer-Coeuret M, Thiounn N, Debre B, Vidal-Trecan G (2000) Risk factors for adult renal cell carcinoma: a systematic review and implications for prevention. BJU Int 86:20–27

Fojo AT, Shen DW, Mickley LA, Pastan I, Gottesman MM (1987) Intrinsic drug resistance in human kidney cancer is associated with expression of a human multidrug-resistance gene. J Clin Oncol 5:1922–1927

Gerloff T, Schaefer M, Johne A, Oselin K, Meisel C, Cascorbi I, Roots I (2002) MDR1 genotypes do not influence the absorption of a single oral dose of 1 mg digoxin in healthy white males. Br J Clin Pharmacol 54:610–616

Goto M, Masuda S, Saito H, Uemoto S, Kikuchi T, Tanaka K, Inui K (2002) C3435T polymorphism in the *MDR1* gene affects the enterocyte expression level of CYP3A4 rather than Pgp in recipients of living-donor liver transplantation. Pharmacogenetics 12:451–457

Hartmann JT, Bokemeyer C (1999) Chemotherapy for renal cell carcinoma. Anticancer Res 19:1541–1544

Hashida T, Masuda S, Uemoto S, Saito H, Tanaka K, Inui K (2001) Pharmacokinetic and prognostic significance of intestinal MDR1 expression in recipients of living-donor liver transplantation. Clin Pharmacol Ther 69:308–316

Hoffmeyer S, Burk O, von Richter O, Arnold HP, Brockmoller J, Johne A, Cascorbi I, Gerloff T, Roots I, Eichelbaum M, Brinkmann U (2000) Functional polymorphisms of the human multidrug–resistance gene: multiple sequence variations and correlation of one allele with P-glycoprotein expression and activity in vivo. Proc Natl Acad Sci 97:3473–3478

Kakehi Y, Kanamaru H, Yoshida O, Ohkubo H, Nakanishi S, Gottesman MM, Pastan I (1988) Measurement of multidrug-resistance messenger RNA in urogenital cancers; elevated expression in renal cell carcinoma is associated with intrinsic drug resistance. J Urol 139:862–865

Kim WJ, Kakehi Y, Kinoshita H, Arao S, Fukumoto M, Yashida O (1996) Expression patterns of multidrug-resistance (MDR1), multidrug resistance-associated protein (MRP), glutathione-S-transferase-π (GST-π and DNA topoisomerase II (TOPO II) genes in renal cell carcinomas and normal kidney. J Urol 156:506–511

Kim RB, Leake BF, Choo EF, Dresser GK, Kubba SV, Schwarz UI, Taylor A, Xie HG, McKinsey J, Zhou S, Lan LB, Schuetz JD, Schuetz EG, Wilkinson GR (2001) Identification of functionally variant *MDR1* alleles among European Americans and African Americans. Clin Pharmacol Ther 70:189–199

Kurata Y, Ieiri I, Kimura M, Morita T, Irie S, Urae A, Ohdo S, Ohtani H, Sawada Y, Higuchi S, Otsubo K (2002) Role of human *MDR1* gene polymorphism in bioavailability and interaction of digoxin, a substrate of P-glycoprotein. Clin Pharmacol Ther 72:209–219

Motohashi H, Sakurai Y, Saito H, Masuda S, Urakami Y, Goto M, Fukatsu A, Ogawa O, Inui K (2002) Gene expression levels and immunolocalization of organic ion transporters in the human kidney. J Am Soc Nephrol 13:866–874

Nakamura E, Megumi Y, Kobayashi T, Kamoto T, Ishitoya S, Terachi T, Tachibana M, Matsushiro H, Habuchi T, Kakehi Y, Ogawa O (2002) Genetic polymorphisms of the interleukin-4 receptor α gene are associated with an increasing risk and a poor prognosis of sporadic renal cell carcinoma in a Japanese population. Clin Cancer Res 8:2620–2625

Rodin SM, Johnson BF (1988) Pharmacokinetic interactions with digoxin. Clin Pharmacokinet 15:227–244

Schaeffeler E, Eichelbaum M, Brinkmann U, Penger A, Asante-Poku S, Zanger UM, Schwab M (2001) Frequency of C3435T polymorphism of *MDR1* gene in African people. Lancet 358:383–384

Schuetz EG, Furuya KN, Schuetz JD (1995) Interindividual variation in expression of P-glycoprotein in normal human liver and secondary hepatic neoplasms. J Pharmacol Exp Ther 275:1011–1018

Siegsmund M, Brinkmann U, Schaffeler E, Weirich G, Schwab M, Eichelbaum M, Fritz P, Burk O, Decker J, Alken P, Rothenpieler U, Kerb R, Hoffmeyer S, Brauch H (2002) Association of the P-glycoprotein transporter $MDR1^{C3435T}$ polymorphism with the susceptibility to renal epithelial tumors. J Am Soc Nephrol 13:1847–1854

Synold TW, Dussault I, Forman BM (2001) The orphan nuclear receptor SXR coordinately regulates drug metabolism and efflux. Nat Med 7:584–590

Tanaka Y, Sasaki M, Kaneuchi M, Fujimoto S, Dahiya R (2002) Single nucleotide polymorphisms of estrogen receptor α in human renal cell carcinoma. Biochem Biophys Res Commun 296:1200–1206

Tanigawara Y, Okamura N, Hirai M, Yasuhara M, Ueda K, Kioka N, Komano T, Hori R (1992) Transport of digoxin by human P-glycoprotein expressed in a porcine kidney epithelial cell line ($LLC\text{-}PK_1$). J Pharmacol Exp Ther 263:840–845

Volm M, Kastel M, Mattern J, Efferth T (1993) Expression of resistance factors (P-glycoprotein, glutathione S-transferase-π, and topoisomerase II) and their interrelationship to proto-oncogene products in renal cell carcinomas. Cancer 71:3981–3987

Wakasugi H, Yano I, Ito T, Hashida T, Futami T, Nohara R, Sasayama S, Inui K (1998) Effect of clarithromycin on renal excretion of digoxin: interaction with P-glycoprotein. Clin Pharmacol Ther 64:123–128

Peptide Transporters: Structure, Function, Regulation and Application for Drug Delivery

Tomohiro Terada and Ken-ichi Inui*

Department of Pharmacy, Kyoto University Hospital, Faculty of Medicine, Kyoto University, Sakyo-ku, Kyoto 606-8507, Japan

Abstract: Proton-coupled peptide transporters, localized at brush-border membranes of intestinal and renal epithelial cells, play important roles in protein absorption and the conservation of peptide-bound amino nitrogen. These transporters also have significant pharmacological and pharmacokinetic relevance to the transport of various peptide-like drugs such as β-lactam antibiotics. The identification and molecular characterization of H^+/peptide cotransporters (PEPT1 and PEPT2) have facilitated the clarification of many aspects of these transporters such as the structure/function relationship and regulation. Recent findings that intestinal PEPT1 can transport L-valine ester prodrugs such as valacyclovir provided a major step forward toward the development of novel drug delivery systems. It has been demonstrated that peptide transporters, which have a similar substrate specificity to PEPT1 and PEPT2, but possess other distinct functional properties, are localized at basolateral membranes of intestinal and renal epithelial cells. This review highlights the recent advances in our knowledge of the cellular and molecular nature of PEPT1, PEPT2 and the basolateral peptide transporters.

1. INTRODUCTION

Dietary protein undergoes a series of degradative steps, resulting in a mixture of free amino acids and small peptides. These products are then taken up by the intestinal epithelial cells and delivered into the circulation [1]. Similarly in the kidney, filtered amino acids and small peptides are efficiently reabsorbed from the proximal tubular cells for conservation of amino acid nitrogen [2].

A large number of studies have provided evidence that the absorption of protein digestion products in the small intestine occurs primarily in the form of small peptides [3]. The transport pathways for small peptides are called peptide transporters. Peptide transporters can accept di- and tripeptides as physiological substrates, indicating that they have a much broader substrate specificity than other nutritional transporters. Consequently, foreign compounds structurally resembling small peptides such as oral β-lactam antibiotics, are recognized by the peptide transporters. Therefore, peptide transporters work not only as nutritional transporters but also as drug transporters (Fig. 1).

Currently, the peptide transporters are divided into two types; i.e., those localized at the brush-border membranes of epithelial cells, and those localized at the basolateral membranes. About a decade ago, two brush-border type peptide transporters were identified, and designated PEPT1 and PEPT2. There are several excellent reviews documenting the molecular nature of PEPT1 and PEPT2 from biochemical aspects to physiological and pharmacological significance [4-9]. In contrast to the brush-border type peptide transporters, little attention has been paid to the basolateral peptide transporters. However, our recent studies have provided unequivocal evidence that the basolateral peptide transporters, which are functionally distinguishable from PEPT1 and PEPT2, are expressed in the intestine and kidney [10-16]. This review deals with the current progress in cellular and/or molecular studies of PEPT1, PEPT2 and the basolateral peptide transporters, as well as with their brief historical background and physiological and pharmacokinetic roles.

2. DRUG TRANSPORT BY PEPTIDE TRANSPORTERS

More than 20 years ago, the clarification of absorption mechanisms for oral β-lactam antibiotics was a very attractive issue in the field of pharmacokinetic research. This is because oral β-lactam antibiotics are efficiently absorbed from the small intestine, although they are ionized at physiological pH and have very low lipid solubility. This completely contradicts the traditional pH-partition theory of drug absorption. Using tissue preparation techniques, various investigators tried to solve this puzzle, and found that these drugs were absorbed by a carrier-mediated system [17-19]. However, it was not clear which carrier was responsible for their absorption. Finally, using intestinal brush-border membrane vesicles, we first provided direct evidence that the orally active β-lactam antibiotics are transported *via* the H^+-coupled peptide transporter [20-21]. Subsequently, transport studies using brush-border mem-brane vesicles and the human intestinal cell line Caco-2, have demonstrated that many peptide-like drugs are absorbed by the H^+-coupled peptide transporter. For example, the anti-cancer agent Bestatin [22], renin inhibitors [23], and several angiotensin converting enzyme (ACE) inhibitors [24] were all reported to be recognized by the peptide transporters.

The transport of peptide-like drugs has also been reported in the kidney. The aminocephalosporin cephalexin was the

*Address correspondence to this author at the Department of Pharmacy, Kyoto University Hospital, Sakyo-ku, Kyoto 606-8507, Japan; Tel: 81-75-751-3577; Fax: 81-75-751-4207; E-mail: inui@kuhp.kyoto-u.ac.jp

1389-2002/04 $45.00+.00 © 2004 Bentham Science Publishers Ltd.

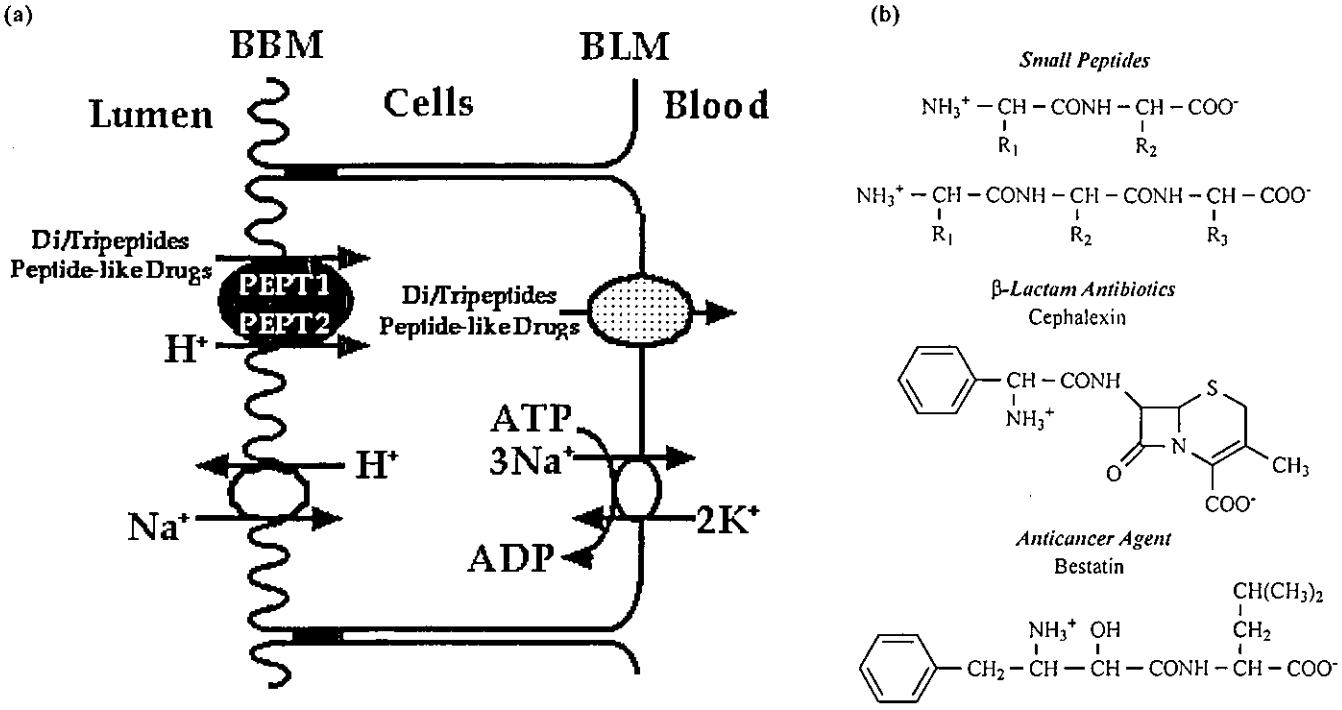

Fig. (1). (a) Peptide transporters in the epithelial cells. BBM, brush-border membranes; BLM, basolateral membranes. (b) Chemical structures of small peptides and peptide-like drugs. Peptide-like drugs structurally resemble di- or tripeptides.

first peptide-like drug whose transport was mediated *via* the renal H^+/peptide cotransporter [25-26]. However, unlike in the intestine, the transport of β-lactam antibiotics in the kidney was mediated by at least two distinct H^+/peptide cotransporters; namely, high affinity-low capacity and low affinity-high capacity transport systems [27-28]. The peptide transport system in the kidney is suggested to be involved in the active transport of these antibiotics from the glomerular filtrate, and to increase their half-life in the circulation.

3. CLONING OF PEPTIDE TRANSPORTERS PEPT1 AND PEPT2

3.1. Structure

A cDNA encoding the H^+/peptide cotransporter (PEPT1) was initially identified by expression cloning using a rabbit small intestinal cDNA library [29]. Homologous cDNAs were then found in human, rat, mouse, cow and chicken [30-34]. As an isoform of the intestinal peptide transporter PEPT1, the renal peptide transporter PEPT2 cDNA has been isolated from human, rabbit, rat and mouse [35-38]. PEPT1 and PEPT2 consist of 707-710 and 729 amino acid residues, respectively, with several putative glycosylation and phosphorylation sites. Hydropathy analysis and an epitope-insertion approach [39] suggested that peptide transporter proteins contain 12 transmembrane domains, with both the C- and N-terminal localized inside the cell. Overall amino acid identity between PEPT1 and PEPT2 is approximately 50%, and the amino acid sequence in the intra- or extracellular loops is more divergent than that in the putative transmembrane regions. The characteristics and putative secondary structure of PEPT1 and PEPT2 are shown in Fig. (2).

3.2. Gene Organization

The human PEPT1 gene is located at chromosome 13q24-q33, consisting of 23 exons, whereas the human PEPT2 gene is located at 3q13.3-q21, consisting of 22 exons. Although there is no report concerning functional promoter analysis of the human PEPT1 and PEPT2 genes, such analyses have been performed using rat [40] and mouse [32] PEPT1 genes and the mouse PEPT2 gene [38]. In the mouse PEPT1 gene, the promoter region upstream of the transcription start site does not contain the TATA box, but possesses three GC boxes. Functional promoter analysis demonstrated that essential promoter/enhancer elements are present within 1,140 base pairs (bp) upstream of the transcription start site. The mouse PEPT2 gene also possesses a TATA-less promoter, and functional promoter analysis revealed that the core promoter region was located between 432 and 286 bp upstream from the translation start site.

It has been reported that single nucleotide polymorphisms of drug transporter genes can affect the pharmacokinetic profiles of drugs [41]. Several polymorphic variants were discovered in the human PEPT1 gene, and suggested the possibility of susceptibility to bipolar disorders [42], but currently, there are no reports on human PEPT1 and PEPT2 gene polymorphism affecting transporter function.

3.3. Tissue Distribution and Membrane Localization

PEPT1 mRNA is mainly expressed in the small intestine and at low levels in the liver and kidney [29-31]. Immunological studies demonstrated that PEPT1 protein is localized to brush-border membranes of the absorptive epithelial cells of the small intestine, and that this protein

(a)

	PEPT1	*PEPT2*
Amino Acids	708~710	729
Identity	100	~50
Tissue Distribution	Small Intestine, Kidney, Liver	Kidney, Brain, Lung, Mammary Gland
Substrates	Di and Tripeptides Peptide-like Drugs Valacyclovir etc.	Di and Tripeptides Peptide-like Drugs δ-Amino Levulinic Acid etc.
Affinity (Km for Gly-Sar)	Low (~1.0 mM)	High (~0.1 mM)
Regulation	Diet, Hormons, Development, Diurnal Rhythm etc.	Chronic Renal Failure etc.

(b)

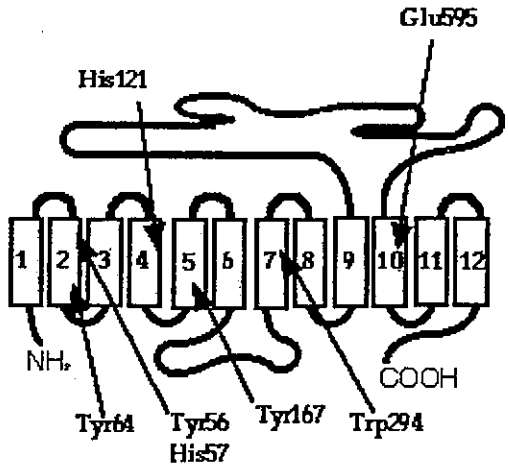

Fig. (2). (a) Summary of PEPT1 and PEPT2. (b) 2nd structure of PEPT1 and PEPT2. The amino acids indicated were putative essential amino acid residues reported by mutagenesis analysis.

was abundant at the tip of the villus and was decreased at the crypt base [43]. In the kidney, PEPT1 protein was localized at the brush-border membranes of the S1 segment of proximal tubules [44]. In the liver, PEPT1 protein is localized at the apical membrane of cholangiocytes of the extrahepatic biliary duct [45]. The physiological and pharmacological significance of PEPT1 in biliary epithelium is currently unclear.

PEPT2 mRNA is predominantly expressed in the kidney, but also in the brain, lung, spleen and mammary gland [35-37]. PEPT2 protein is localized at the brush-border membranes of the S3 segment of proximal tubules [44]. The different intrarenal distributions of PEPT1 and PEPT2 may contribute to the efficient reabsorption of small peptides, and reflects the previous finding that transport of β-lactam antibiotics in the kidney was mediated by at least two distinct H^+/peptide cotransporters [27-28]. In the brain, *in situ* hybridization studies have demonstrated that PEPT2 mRNA is expressed by astrocytes, subependymal cells, ependymal cells and epithelial cells of the choroid plexus [46]. Immunological analysis showed that PEPT2 protein is expressed in satellite glial cells surrounding the ganglionic neurons [47] and present at the apical membranes of choroidal epithelial cells [48]. In the lungs, PEPT2 protein was expressed in alveolar type II pneumocytes, bronchial epithelium, and endothelium of small vessels [49]. In the mammary gland, PEPT2 protein was expressed in epithelial cells of the gland and duct [50]. The function of PEPT2 in the choroid plexus, lung and mammary gland was also confirmed by using various tissue preparation techniques [48-50], and hence PEPT2 has been suggested to play important roles in drug delivery and disposition in these tissues. Very recently, Shen *et al.* [51] have developed *PEPT2*-deficient mice, which were viable and without obvious kidney or brain abnormalities. Using isolated choroid plexus from $PEPT2^{-/-}$ mice, they have clearly demonstrated that $PEPT2^{-/-}$ mice show impaired uptake of dipeptide in the choroid plexus, and have suggested that *PEPT2* is the primary member of the peptide transporter family responsible for the trafficking of peptides/mimetics at the blood-cerebrospinal fluid barrier [51].

4. FUNCTIONAL CHARACTERISTICS OF PEPT1 AND PEPT2

4.1. Substrate Specificity

Both PEPT1 and PEPT2 can transport di- and tripeptides with different molecular sizes and charges, but not free amino acids and tetrapeptides [29, 36]. Pharmacologically active peptide-like drugs such as β-lactam antibiotics, Bestatin and ACE inhibitors have been also reported to be transported by PEPT1 and PEPT2 [31, 37, 52-54]. Recently, it has been demonstrated that the bacteria-derived chemotactic peptide (*N*-formylmethionyl-leucyl-phenylalanine (fMLP)) is transported by intestinal PEPT1, and suggested that fMLP transport by PEPT1 induces intestinal inflammation [55-57].

It is believed that the presence of peptide-bond(s) is the most important factor in the recognition of substrates by peptide transporters. However, structural requirements of PEPT1 and PEPT2 were re-evaluated (most studies were performed in PEPT1), and it was demonstrated that even compounds without peptide bond(s) can be accepted as substrates. For example, 4-aminophenylacetic acid [58], δ-amino levulinic acid [59], ω-amino fatty acid [60], amino

acid aryl amide [61], and valacyclovir [62] can be accepted as substrates. From the pharmaceutical standpoint, the finding of valacylcovir transport by PEPT1 can provide new strategies for drug delivery, and this topic will be discussed in Kunta *et al.* (this issue). Interestingly, some peptide mimetic drugs such as the ACE inhibitor quinapril and the anti-diabetic agent glibenclamide showed noncompetitive inhibition of PEPT1 and PEPT2 [63-65]. These findings and data obtained in different expression systems have been used for modeling to obtain a template for the interaction within the substrate-binding domain [66].

4.2. Substrate Affinity

Functional expression studies have clearly established that PEPT1 is a low-affinity transporter, whereas PEPT2 is a high-affinity transporter. For example, PEPT2 showed higher affinity for chemically diverse dipeptides and tripeptides compared to PEPT1 [67]. PEPT2 also exhibited higher affinity for amino β-lactam antibiotics [68]. These differences in substrate affinity are not necessarily limited to substrates with peptide bond(s). Nonpeptidic compounds such as valacyclovir and δ-amino levulinic acid are preferentially recognized by PEPT2 rather than PEPT1 [69]. Notably, anionic β-lactam antibiotics such as ceftibuten [68] and 8 amino-octanoic acid [69] showed higher affinity for PEPT1 than for PEPT2. A feature of these compounds is the lack of α- or β-amino carbonyl function, thus, it has been suggested that the α- or β-amino carbonyl function is a key structure in exhibiting higher affinity for PEPT2 than for PEPT1 [69-70].

4.3. Stoichiometry

PEPT1 and PEPT2 can transport a wide variety of substrates in an electrogenic mode as a consequence of H^+ and substrate cotransport. These electrogenic characteristics of PEPT1 and PEPT2 are commonly observed, but it has been unclear how carrier proteins can transport differently charged substrates in the same general transport mode.

Several studies have shown that the transport of zwitterionic dipeptides by PEPT1 is electrogenic, and this occurred at a proton-to-substrate flux coupling ratio of 1:1 [29, 71-73]. Cationic dipeptides can be transported in neutral and positively-charged forms, resulting in excess transport current as compared to neutral substrates [71, 73]. On the other hand, in the case of anionic dipeptides, the situation is more complicated, and several hypotheses have been suggested as follows. 1) Electrogenic transport of anionic dipeptides may be due to the cotransport of one substrate molecule together with two protons [72-74], or 2) it could result from the cotransport of one proton per substrate molecule and a simultaneous countertransport of one negatively-charged counterion such as OH^- or HCO_3^- [71]. 3) An alternative explanation could be the preferential transport of only the zwitterionic form of the substrate with one proton [75-76]. So, the stoichiometry of anionic dipeptides to H^+ is still controversial, and may be caused by these mixed effects. In the case of PEPT2, a proton to substrate stoichiometry of 3:1 was proposed for the influx of dipeptides [77]. As many studies have been performed using dipeptides, there is limited information available about the stoichiometry of peptide-like drugs to H^+ [75].

4.4. Structure/Function Relationship Analysis

To fully exploit PEPT1 (also PEPT2) for optimizing drug delivery, it will be necessary to understand its substrate recognition mechanisms. After the cloning of PEPT1 and PEPT2 cDNAs, several approaches have been used to clarify their substrate binding domains by protein engineering methods and computer modeling analyses.

Using a site-directed mutagenesis technique, it has been shown that the conserved histidine (His57 and His121) and tyrosine (Tyr56, Tyr64 and Tyr167) residues in the second, fourth and fifth transmembrane domain (TMD) of PEPT1 and PEPT2 are essential for the transport activity and/or substrate binding [78-81] (Fig. 2). One histidine residue was suggested to be the binding site for an α-amino group of substrates [82], and another was an H^+-binding site [81-82]. As described below, based on computational modeling, Bolger *et al.* [83] reported that the mutation of Trp294 or Glu595 in human PEPT1 reduced glycylsarcosine (Gly-Sar) uptake by 80 and 95%, respectively (Fig. 2).

The second approach is the analysis of chimeric PEPT1/PEPT2 proteins. Döring *et al.* [84] first constructed a chimeric peptide transporter with rabbit PEPT1 and PEPT2 and compared its functions with those of the parent transporters. They demonstrated that the phenotypic characteristics of PEPT2 were determined by its amino-terminal region (TMD1~9), suggesting that the large extracellular loop between TMD9 and TMD10, comprising one-third of the transporter protein, might not be responsible for substrate binding [84]. Following PEPT1/PEPT2 chimera studies from various groups, narrower segments responsible for substrate binding and other functional properties have been identified [85-86]. According to the recent report of Döring *et al.* [87], the first 59 amino acid residues up to the second TMD may form an important part of the substrate-binding domain in peptide transporters.

The third approach is computer modeling. Through the iterative process (from computational modeling to functional assay), it was predicted that the substrate binding domain of human PEPT1 was composed of Tyr12 and Glu26 from TMD1, Tyr91 from TMD3; Tyr167 from TMD5; Trp294 and Arg282 from TMD7; Asp341 from TMD8 and Tyr588 and Glu595 from TMD10 [83].

All three approaches provide important information about the structure/function relationship of peptide transporters. However, it should be noted that all of the functional residues and domains described here are not completely correlated with each other. Further studies will be needed to clarify how PEPT1 and PEPT2 recognize and transport various substrates.

4.5. Regulation

It has been reported that intestinal PEPT1 activity is physiologically regulated by various factors including dietary conditions [40, 88-89], hormones (insulin, leptin and thyroid hormone) [90-93], growth factor (epidermal growth factor) [94], development [95-97] and diurnal rhythm [98]. As well as physiological factors, PEPT1 is regulated by pharmacological agents such as σ-receptor ligand (+)-pentazocine [99] and α_2-adrenergic agonists [100]. The